A99-24626

AIAA-99-1233

ADDITIONAL BUCKLING SOLUTIONS IN PANDA2

David Bushnell[1] , Senior Staff Scientist, retired, Dept. H1-61, Bldg. 250
Lockheed Martin Advanced Technology Center
3251 Hanover St., Palo Alto, California 94304

Hao Jiang , Graduate Student, and Norm F. Knight, Jr[2]., Professor
Aerospace Engineering Department, Old Dominion University, Norfolk, Virginia

ABSTRACT

Three new buckling models have been incorporated into PANDA2, a program for minimum weight design of stiffened composite panels and shells: 1. buckling of unstiffened panels or unstiffened portions of panels with use of double-trigonometric series expansions for buckling modal displacement components, *u, v, w*; 2. general buckling of cylindrical, stiffened panels with both rings and stringers treated as discrete beams; and 3. inter-ring buckling of cylindrical panels based on a discretized single module model containing discretized ring segments and a discretized skin-smeared-stringer cylindrical surface to which the ring is attached. Examples are provided of buckling of certain isotropic and laminated composite flat and cylindrical unstiffened and stiffened panels and shells for which the predictions from the modified PANDA2, formerly unacceptably inaccurate, are compared with predictions from STAGS, a general-purpose finite element code. The new comparisons demonstrate that the modified PANDA2 is now well qualified for preliminary design in particular cases for which it previously yielded unreliable designs and designs that were overly conservative. The optimum design of a composite ring and stringer stiffened cylindrical shell derived by PANDA2 is evaluated with use of STAGS. The optimum design of an isotropic hydrostatically compressed internally T-ring stiffened cylindrical shell optimized by PANDA2 is evaluated with use of the shell-of-revolution code BOSOR4. There is good agreement between PANDA2 predictions and STAGS and BOSOR4 predictions for buckling of the optimized designs.

INTRODUCTION

PANDA2, a program for minimum weight design of stiffened panels and shells, has been under development since the early 1980's [1,2]. Brief surveys of previous work on buckling and optimization of stiffened panels and shells appear in [1], the most recent in AIAA Paper 98-1990. Therefore, no additional survey will be included here.

Previously PANDA2 included the following buckling models:

1. A discretized single skin-stringer module of the type shown in Fig. 1, for example. This model is used for local buckling, local postbuckling, and wide column buckling of the panel region between adjacent rings (transverse stiffeners).

2. Simple models for the buckling of the panel skin and stiffener segments of the type described in [2]. Typical buckling modes of the panel skin and stiffeners are shown in Fig. 6 of [2] and Fig. 180 on p. 209 of [27]. In the panel skin the buckling nodal lines are assumed to be straight, as shown in Fig. 2. This type of buckling model is used in some of the software written by Arbocz and Hol [3] and by Khot and his colleagues [4-6]. These models are called "PANDA-type (closed form)" in PANDA2 jargon because they are the only ones used in the original PANDA program [2], which is superseded by PANDA2 [1].

[1]Fellow, AIAA; email: bush@trinity.atc.lmco.com

[2]Associate Fellow, AIAA, presently at MRJ Technology Solutions, Yorktown, VA

Now three new buckling models have been added to PANDA2, as follows:

1. local buckling between adjacent stringers and rings of a cylindrical or flat panel obtained from a Ritz model in which the buckling modal displacement components, *u, v, w,* are expanded in double trigonometric series. The local region is assumed to be simply supported on all four edges.

2. general buckling of a cylindrical panel in which stringers and rings are treated as discrete beams with undeformable cross sections. Again, the general buckling modal displacement components, *u, v, w,* are expanded in double trigonometric series. The edges of the domain are assumed to be simply supported and to have discrete stiffeners of half the user-specified modulus. The domain for this model is usually a subdomain of the entire panel.

3. a discretized single module model for a cylindrical panel in which the RING segments and panel skin-with-smeared-stringers are discretized as shown in Fig. 1. Until now, the only discretized module model in PANDA2 involved the panel skin and STRINGER segments. The RINGS were "second-class citizens". In this "branched shell" model the cross sections of the stiffeners can deform in the buckling mode, since they are subdivided into finite elements of the type used in BOSOR4 [28].

NEW "ALTERNATE" LOCAL BUCKLING MODEL FOR FLAT OR CYLINDRICAL PANELS

Introduction

The new alternate solution is needed for nearly square flat or cylindrical panels subjected to significant in-plane shear loading and flat or cylindrical composite laminates with significant anisotropic terms, B_{16}, B_{26}, or D_{16}, D_{26}, such as occur especially in angle-ply laminates with few layers. In addition, the new alternate solution will compute general instability load factors for stiffened panels in which the stiffeners are modeled as discrete. The new "discrete stiffener" capability is discussed in the next major section. This section deals only with unstiffened panels or the unstiffened portion of a panel between adjacent stiffeners.

In this section two "PANDA-type" solutions are referred to:

1. The "original" PANDA-type solution. This is the solution based on the one-term Ritz formulation given as Eqs. (50,57) in [2]. Buckling in the panel skin has straight nodal lines, as shown in Fig. 2. PANDA2 selects either the buckling model depicted in Fig. 2a or that depicted in Fig. 2b, depending on the dimensions, ratios of axial to transverse bending stiffnesses, and curvature. In some of the sample problems explored in this paper there is an unacceptably large discontinuity in buckling load factor in the transition from the buckling model in Fig. 2a to that in Fig. 2b. The existence of this large discontinuity provided one of the main motivations for the introduction into PANDA2 of the new buckling solutions based on double trigonometric series expansions for buckling modal displacement components, *u, v, w.*

2. The "alternate" solution. The alternate solution involves double trigonometric series expansions of the buckling modal displacement components, *u, v, w.* The "alternate" solution is of the type described by Timoshenko [7], by Whitney (pp 152-156 of [8], by Jones [9], by Simitses [10,11], by Jaunky, Knight and Ambur [12,13] and by others.

The new branch was developed and inserted into PANDA2 after some exploratory studies [14] revealed that PANDA2 yielded unacceptably poor predictions of linear bifurcation buckling load factors for certain composite, angle-ply, flat, square, simply supported plates under uniform axial compression. In particular, the PANDA2 predictions in [14] were compared with predictions of Whitney for a one-layered $[+\theta]_{total}$ square plate and predictions of Jones [9] for two-layered $[+\theta,-\theta]_{total}$ and four-layered $[+\theta, -\theta, -\theta, +\theta]_{total}$ angle-ply, square, simply supported plates under uniform axial compression. Mr. Jiang [14] found that PANDA2's predictions were too conservative in the case of the one-layered plate for layup angle θ less than about 60 degrees and were unacceptably unconservative in the case of the two-layered plate over the range of layup angles from about 10 to about 80 degrees. The four-layered plate behaved in a manner similar to the one-layered plate: PANDA2's predictions were overly conservative for layup angle less than about 45 degrees and there was an abrupt, unacceptably large, increase in buckling load at the layup angle for which the original PANDA-type model perceives the need for a transition from one model of buckling, shown in Fig. 2(b) to another model of buckling, shown in Fig. 2(a).

Predictions for square axially compressed flat plates from PANDA2's original closed form solution improve

as the number of alternating (+θ,-θ) pairs of plies increases, that is, as the anisotropic elements, D_{16} and D_{26} (called C_{46} and C_{56} in PANDA2 jargon), become smaller relative to the orthotropic bending stiffness components, D_{11} and D_{22} (C_{44} and C_{55} in PANDA2 jargon) [19]. Also, predictions from PANDA2's original closed form solution for rectangular plates under pure in-plane shear loading improve as the plate aspect ratio becomes significantly larger than unity or smaller than unity, provided the panel has more than two layers (is not of the type $[+\theta, -\theta]_{total}$). It has long been known that PANDA2's predictions of buckling of nearly square plates under pure in-plane shear, N_{xy}, has been too conservative.

One-layer and two-layer composite laminates are not common in practical plates and shells. Therefore, one might conclude that PANDA2's failure to predict buckling accurately in these cases is of little significance. However, PANDA2's original predictions in the case of axially compressed plates with a four layered symmetric layup, $[+\theta, -\theta, -\theta, +\theta]_{total}$, are of poor quality for nearly square plates with layup angles less than about 45 degrees. Such plates might occur in very lightweight structures. Also, the relatively poor predictions of PANDA2 for buckling of plates under uniform in-plane shear loading, N_{xy}, even in the case of isotropic plates, provides motivation to include a better solution for linear bifurcation buckling in the PANDA2 "stable" of buckling models as an alternate to the one-term Ritz model described in [2] and shown in Fig. 2.

New input datum required in "MAINSETUP/PANDAOPT"

In the case of the new alternate solution, for adequate convergence of buckling load factor with respect to number of terms taken in the double trigonometric series expansions for buckling modal displacement components, u, v, w, it is necessary to extract eigenvalues from "full" matrices with rank of up to 125. The formation of the stiffness and load-geometric matrices and the extraction of eigenvalues for such systems of linear equations requires much more computer time than does the original one-term Ritz model. Therefore, the PANDA2 user is now given the choice of whether he or she wants to employ the "alternate" solution. Hence, there is a new input datum required during the MAINSETUP interactive session. This new "y" or "n" response is in reply to the new prompting question,

"Do you want to use the "alternate" buckling solution?"

which now immediately follows the prompt that refers to mode jumping.

Table 1 lists the additions to the ..panda2/execute/PROMPT.DAT file, which provides the prompting questions and "help" paragraphs for PANDA2 input data. NOTE: Old PANDA2 input files with the name *.OPT will no longer work with the new version of PANDA2 because of this new input datum.

Theory

The new alternate buckling theory is based on the following:

1. The assumed buckling modal displacement field for axial displacement u, circumferential (hoop) displacement v, and normal displacement w are:

$$\begin{aligned} u &= \sum_{m}^{m_{max}} \sum_{n}^{n_{max}} \begin{bmatrix} A(m,n)\cos(\overline{m}x)\sin(\overline{n}y) \\ +D(m,n)\sin(\overline{m}x)\sin(\overline{n}y) \end{bmatrix} \\ v &= \sum_{m}^{m_{max}} \sum_{n}^{n_{max}} \begin{bmatrix} B(m,n)\sin(\overline{m}x)\cos(\overline{n}y) \\ +E(m,n)\sin(\overline{m}x)\sin(\overline{n}y) \end{bmatrix} \\ w &= \sum_{m}^{m_{max}} \sum_{n}^{n_{max}} \left[C(m,n)\sin(\overline{m}x)\sin(\overline{n}y) \right] \end{aligned} \tag{1a}$$

in which $\overline{m}$ and $\overline{n}$ are wave indices given by

$$\begin{aligned} \overline{m} &= m\pi / x_{max} \\ \overline{n} &= n\pi / y_{max} \end{aligned} \tag{1b}$$

where m and n are the number of halfwaves in the axial direction x and circumferential direction y, respectively, and x_{max} is the axial length of the panel or portion of it being analyzed, and y_{max} is the circumferential arc length of the panel or portion of it being analyzed.

Note that the series expansions for in-plane displacement components, u and v, contain terms with $D(m,n)$ and $E(m,n)$, respectively. These series expansions are required for cylindrical panels and for flat or cylindrical panels involving significant anisotropic terms, B_{16} and B_{26} (called C_{16} and C_{26} in PANDA2 jargon).

2. The kinematic (strain-displacement) relations are:

$$e_x = u_{,x} \qquad e_y = v_{,y} + w/r \qquad e_{xy} = u_{,y} + v_{,x}$$
$$k_x = -w_{,xx} \qquad k_y = -w_{,yy} + v_{,y}/r$$
$$k_{xy} = 2\left(-w_{,xy} + v_{,x}/r\right) \tag{2}$$

in which r is the radius of the cylindrical panel.

3. The strain energy is given by:

$$U = \frac{1}{2}\int_x\int_y \mathbf{e}^T\mathbf{C}\mathbf{e}\, dydx \tag{3a}$$

in which

$$\mathbf{e}^T = \begin{bmatrix} e_x & e_y & e_{xy} & k_x & k_y & k_{xy} \end{bmatrix} \tag{3b}$$

and $\mathbf{C}$ is the usual 6x6 symmetric matrix of stiffness coefficients that represents the constitutive law as integrated through the wall thickness.

Donnell [16] and Sanders [17] theories:

4. The work done by prebuckling in-plane loads, N_x, N_y, N_{xy}, during bifurcation buckling modal displacements (from Sanders theory [17]) is given by:

$$W = \frac{1}{2}\int_x\int_y \begin{bmatrix} N_x\left(w_{,x}^2 + \gamma^2\right) \\ +N_y\left(\left(w_{,y} - v/r\right)^2 + \gamma^2\right) \\ +N_{xy}w_{,x}\left(w_{,y} - v/r\right) \end{bmatrix} dydx \tag{4}$$

in which

$$\gamma = \frac{1}{2}(u_{,y} - v_{,x}) \tag{5}$$

5. The "work done", W, can be expressed in a form analogous to that used for the strain energy. If we define three rotation components, r_x, r_y, r_{xy}, as follows:

$$r_x = w_{,x} \qquad r_y = w_{,y} - v/r \qquad r_{xy} = \frac{1}{2}\left(u_{,y} - v_{,x}\right) \tag{6}$$

6. then the "work done", W, is given by

$$W = \frac{1}{2}\int_x\int_y \mathbf{r}^T\mathbf{N}\mathbf{r}\, dydx \tag{7}$$

in which

$$\mathbf{r}^T = \begin{bmatrix} r_x & r_y & r_{xy} \end{bmatrix}$$

and the 3x3 matrix $\mathbf{N}$ is given by:

$$\mathbf{N} = \begin{bmatrix} N_x & N_{xy} & 0 \\ N_{xy} & N_y & 0 \\ 0 & 0 & N_x + N_y \end{bmatrix} \tag{8}$$

in which N_x, N_y, N_{xy}, are the applied axial, circumferential, and in-plane shear resultants, respectively.

Marlowe theory [18]:

7. The work done by prebuckling in-plane loads N_x,N_y, N_{xy}, during bifurcation buckling displacements (from Marlowe theory [18]) is given by:

$$W = \frac{1}{2}\int_x\int_y \begin{bmatrix} N_x\left(\chi^2 + \gamma_1^2 + \gamma_{21}^2\right) \\ +N_y\left(\psi^2 + \gamma_2^2 + \gamma_{12}^2\right) \\ +N_{xy}\left(\chi\psi + \gamma_1\gamma_{12} + \gamma_2\gamma_{21}\right) \end{bmatrix} dydx \tag{9}$$

in which

$$\chi = w_{,x} \qquad \psi = w_{,y} - v/r \qquad \gamma_1 = u_{,x}$$
$$\gamma_2 = v_{,y} + w/r \qquad \gamma_{12} = u_{,y} \qquad \gamma_{21} = v_{,x} \tag{10}$$

8. We wish to express the "work done", W, in a form analogous to that used for the strain energy. If we define a vector $\mathbf{r}$ with the six components,

$$\mathbf{r}^T = \begin{bmatrix} \chi & \psi & \gamma_1 & \gamma_2 & \gamma_{12} & \gamma_{21} \end{bmatrix} \tag{11}$$

9. then the "work done", W, is given by

$$W = \frac{1}{2}\int_x\int_y \mathbf{r}^T\mathbf{N}\mathbf{r}\, dydx \tag{12}$$

in which $\mathbf{N}$ is a 6 x 6 matrix given by:

$$\mathbf{N} = \begin{bmatrix} N_x & N_{xy} & 0 & 0 & 0 & 0 \\ N_{xy} & N_y & 0 & 0 & 0 & 0 \\ 0 & 0 & N_x & 0 & 0 & N_{xy} \\ 0 & 0 & 0 & N_y & N_{xy} & 0 \\ 0 & 0 & 0 & N_{xy} & N_x & 0 \\ 0 & 0 & N_{xy} & 0 & 0 & N_y \end{bmatrix} \quad (13)$$

Eigenvalue extraction:

Eigenvalues are extracted via a "mathpak" subroutine called GSEIG, which begins with the following description:

"GSEIG solves the small, full, generalized, symmetric eigenproblem

$$\mathbf{Ax} - \lambda \mathbf{Bx} = \mathbf{0}. \quad (14)$$

A generalized Jacobi iteration is simultaneously applied to the matrices **A** and **B** until they are diagonalized. The process will fail if and only if the given problem has complex eigenvalues."

Discussion

The following overall properties of the new alternate solution are emphasized:

1. The (*u, v, w*) formulation is used rather than the frequently cited (*w, f*) formulation, in which *f* is a stress function used in the shallow shell (Donnell [16]) approximation. The "*u, v, w*" formulation is required because the alternate solution is programmed for the Sanders [17] and Marlowe [18] shell theories in addition to the Donnell theory.

2. If the plate is flat and has a balanced laminate (no B_{16}, B_{26} terms), then the Timoshenko [7] and Whitney [8] model is used, that is, only the trigonometric series expansion for buckling modal displacement component *w* is required. In this case PANDA2 uses a maximum of 11 as the upper limits, m_{max} and n_{max} on number of axial halfwaves (m) and number of circumferential half waves (n) in the double trigonometric series expansion for normal displacement *w*. If, on the other hand, displacement components *u* and *v* are required, then PANDA2 uses upper limits, $m_{max} = n_{max} = 5$ on all of the trigonometric series expansions during an initial search for a critical buckling load factor (see No. 5 just below) and upper limits $m_{max} = n_{max} = 7$ (except as noted below) on all of the trigonometric series expansions during the final evaluation for the current design and during all design perturbations. Advantage is taken of the fact that, provided the anisotropic B_{16} and B_{26} terms are not significant, the total system of equations $\mathbf{Ax} = \lambda \mathbf{Bx}$ can be split into two smaller systems of equations of approximately half the total rank each. In one of the subsystems m + n is odd (m = number of axial halfwaves; n = number of circumferential halfwaves) and in the other m + n is even. The alternate solution is obtained much faster and requires less storage if the split into m+n=odd and m+n=even subsytems can be introduced. If, because of significant "B_{16} or B_{26}" anisotropy, $\mathbf{Ax} = \lambda \mathbf{Bx}$ cannot be split into "odd" and "even" subsystems, then the upper limit on trigonometric series expansions for *u, v, w,* is maintained at 5 and NOT increased to 7 for cases in which in-plane displacement components *u* and *v* are present.

3. IALTSN is the user-provided switch for use (IALTSN = 1) or non-use (IALTSN = 0) of the alternate solution. If the user sets IALTSN = 1, then PANDA2 will override the user's wishes under the following circumstances, that is, PANDA2 will NOT use the alternate solution if:

3a. The panel is very long in the axial direction compared to the circumferential direction and B_{16}, B_{26} anisotropic terms are not significant.

3b. The panel is very long in the circumferential direction compared to the axial direction and B_{16}, B_{26} anisotropic terms are not significant.

3c. There is no significant applied in-plane shear loading N_{xy} and the panel wall is not significantly anisotropic (A_{13}, A_{23}, B_{16}, B_{26}, D_{16}, D_{26} are small [19]).

3d. The panel is cylindrical and the critical buckling mode from the original PANDA-type solution has more than three circumferential halfwaves.

3e. There is no significant B_{16}, B_{26} anisotropy and the absolute value of the nodal line slope of the critical buckling mode from the original PANDA-type solution is either very small or very large, that is, if the original PANDA-type solution yields a critical buckling mode that has approximately the "classical checkerboard" pattern.

3f. If the "high-m" buckling load factor (see ITEMs 415

and 443 in [15] and Table 2 in this paper) from the original PANDA-type theory is larger than the "low-m" buckling load factor, and if this "high-m" buckling load factor is smaller than that obtained from the alternate solution, then PANDA2 uses the "high-m" buckling load factor from the original PANDA-type theory rather than the buckling load factor from the alternate solution.

4. Note that there are rather small upper limits, m_{max} and n_{max} on number of axial (m) and number of circumferential (n) halfwaves to be used in the double trigonometric series expansions (1a,b), especially in cases involving non-trivial in-plane displacement components u and v for which the upper limit is only five during the initial searching phase of the analysis. This limitation generates a requirement for some fancy strategy for panels that are much longer in one direction than the other (but not so long that PANDA2 elects not to perform the alternate solution), especially for cylindrical panels that are long in the axial direction, such as might well be the case for local skin buckling of a cylindrical stringer-stiffened panel. Straightforward application of the series expansions to the actual panel would result in unacceptably unconservative buckling load factors because of lack of convergence with respect to number of trigonometric terms used in the solution, in particular the number of terms used for the x-coordinate series expansions. As is typical in applications of the Ritz model, the buckling load factor converges from above, that is, more and more trigonometric terms in the series expansions for u,v,w yield a converging series of lower and lower buckling load factors. The use of too few terms results in too high (unconservative) predictions. Therefore, in the case of panels with high aspect ratios, PANDA2 obtains, at the current design, multiple alternate solutions for various sublengths of panel with the upper limits, m_{max} and n_{max}, held at five. When the most critical sublength has been established in this manner, the alternate solution is obtained once more, this final time with the upper limits, m_{max} and n_{max}, set at seven rather than five. The critical buckling load factor for the current design is that determined by this final analysis with the upper limits, m_{max} and n_{max}, set at seven. For each design PERTURBATION, the upper limits, m_{max} and n_{max}, are held at seven and there is no search for a perturbed critical sublength. See Table 2 and the discussion in the subsection entitled "Digression...".

NOTE: In cases of panels with significant "B_{16}, B_{26}" anisotropy, that is, cases for which the equation system, $\mathbf{Ax} = \lambda\mathbf{Bx}$, cannot be split into two decoupled (m+n)=odd and (m+n)=even subsets, the upper limits. m_{max} and n_{max}, in Eqs. (1a) are maintained at five and NOT increased to seven. This is done because of limitations on storage and computer time required to solve the fully coupled eigenproblem.

5. At the UNPERTURBED (current) design in each optimization cycle, the critical buckling load factor (smallest positive eigenvalue) is obtained via SUBROUTINE GSEIG, which is a "mathpak" routine based on generalized Jacobi iteration. For each PERTURBED design (same as the unperturbed design except that one decision variable is changed by a small amount; the perturbed designs are used to obtain gradients of the behavioral constraint conditions during optimization cycles) the critical buckling load factor is obtained from the Rayleigh quotient:

$$\text{eigenvalue} = \lambda = \frac{\Phi^T \mathbf{A} \Phi}{\Phi^T \mathbf{B} \Phi} \tag{15}$$

in which Φ is the buckling mode computed for the UNPERTURBED design, $\mathbf{A}$ is the stiffness matrix corresponding to the PERTURBED design, and $\mathbf{B}$ is the load-geometric matrix corresponding to the PERTURBED design.

6. If IQUICK = 0 (PANDA2 user has indicated in MAINSETUP that he/she wants to use the discretized skin-stringer module model for local buckling [1]), then PANDA2 needs the alternate solution only to refine the knockdown factor employed in the derivation of a buckling load factor from the discretized model. This knockdown factor compensates for anisotropy and in-plane shear loading, both of which are not directly involved in the discretized solution, since that solution is based on a BOSOR4-type model [28] in which anisotropy and in-plane shear loading are neglected.

NOTE: the discretized module model is based on the approximation that the panel between adjacent stringers is flat, whereas the alternate solution retains the curvature of the panel if there is any.

7. Knockdown factors for initial geometric imperfections are derived without use of the alternate solution. The section of PANDA2 in which imperfection sensitivity is calculated [20] remains unchanged.

8. The KOITER (local postbuckling) branch of PANDA2 [21] remains unchanged, that is, the displacement field assumed in the local postbuckling

analysis is still given by Eq. (12) on p. 52 of [21]. Stresses in the various segments of the discretized panel module are computed in the KOITER branch. Hence, the new alternate solution does not affect stress constraints.

9. All the computations that involve calls to SUBROUTINEs BUCPAN and GENSTB (PANDA-type buckling load factors are derived in GENSTB) for the purposes of deriving the effective length of a clamped panel and for the purpose of deriving effective overall axial bending stiffness of a precompressed panel (used for determination of overall bending behavior of a flat axially compressed panel under normal pressure) do NOT employ the alternate solution. These computations, based on the original PANDA-type closed form approximation [2], remain unchanged.

10. PANDA2 derives, from the original closed-form PANDA-type theory (in SUBROUTINEs BUCPAN and GENSTB) local buckling load factors for panels including the "rolling of stiffeners with participation of the panel skin". These PANDA-type buckling load factors are now modified (if IALTSN = 1, that is, if the user elects to employ the alternate buckling solution) by suitable application of the ratio of buckling load factors,

$$\text{ratio} = \text{EIGALT} / \text{EIGPAN} = \frac{(\text{eigenvalue from alternate solution})}{(\text{eigenvalue from original solution})} \qquad (16)$$

in which the "alternate soln" and "original soln" are those for the panel skin between adjacent stringers and rings as if that panel segment were simply supported along all four of its edges. In other words, the "alternate solution" introduced into PANDA2 in the "local rolling with skin participation" section of SUBROUTINE BUCPAN of PANDA2 does NOT DIRECTLY include the contribution of attached stiffeners to the strain energy or work done by prebuckling forces during buckling deformations. (However, please see the next major section of this paper for further improvements with regard to application of the new alternate solution to panels with attached stiffeners that are treated as discrete.) The alternate solution as described in this major section of this paper is strictly valid ONLY for panels simply supported along all four edges. Adjustment of the local buckling modes entitled "rolling of stiffeners with participation of panel skin" via the ratio given in Eq. (16) represents an approximation.

11. The t.s.d. (transverse shear deformation) effect is accounted for in the same manner as in the rest of PANDA2: The eigenvalue from the alternate solution, which corresponds to a Kirchhoff model, is "knocked down" by a factor derived from a model analogous to Timoshenko beam theory. This "knocking down" is performed in SUBROUTINE SHRRED. The t.s.d. model remains unchanged. It is described in Section 8.2 (pp 495-496) of [1].

12. A "knockdown" factor of 0.95 is applied to the alternate local buckling load factor in order to compensate for truncation of the double trigonometric series expansions at five or seven halfwaves in each coordinate direction and in order to compensate for an incomplete search over various sublengths of panel. The factor of 0.95 was arrived at as a result of many comparisons between PANDA2 and STAGS during the development of the new alternate buckling solution.

For details concerning the theory and implementation of the alternate solution, please read the comments and study the algorithms listed in Tables 438.2 and 438.3 of [15]. Also see Table 2 of this paper and the discussion associated with Table 2 in the subsection entitled "Digression".

Numerical Results

All results in this section correspond to the panel being simply supported along all four edges. The effect of transverse shear deformation (t.s.d.) is included in all cases. In the legends at the top of the plots the string "DONL" means "Donnell theory used" and the string "SAND" means "Sanders theory used".

Flat Plates

Figures 3 - 13 show results from buckling analyses of flat plates with the old version of PANDA2 [1] and with the modified PANDA2 and with STAGS [22, 23].

In Fig. 3, which shows a buckling load-interaction curve for a square, isotropic, flat aluminum (modulus E=10 msi, $\nu = 0.3$) 10-inch plate with thickness t = 0.1 inch under combined axial compression N_x and in-plane shear loading N_{xy}, the PANDA2 results corresponding to the new alternate solution fall slightly inside the STAGS predictions because the buckling load factor from the alternate solution in PANDA2 is arbitrarily

"knocked down" by a factor of 0.95 in order to compensate for possible lack of convergence with respect to the number of terms used for the trigonometric expansions given in Eq. (1a,b). In this case in-plane buckling modal displacement components, u and v, play no role. The upper limit on m and n [m=number of axial (x) halfwaves; n=number of "circumferential" (y) halfwaves] is 11. The original PANDA-type solution ([2], small squares) is increasingly conservative as the proportion of in-plane shear loading N_{xy} increases.

Figures 4 - 6 show buckling loads for 10-inch square, flat, angle-ply, composite plates under uniform axial compression, N_x = -1.0 lb/in as a function of layup angle, ANG(1). (Material properties: E_{11} = 29.6 msi, E_{22} = 2.96 msi, G_{12}=G_{13}=0.740 msi, G_{23}=0.5328 msi, ν_{minor}=0.03). Layup angle, ANG(1) = 0 degrees, corresponds to the ply fibers being aligned with the axial coordinate, x. All three figures correspond to a total laminate thickness, t = 0.1 in. In each of the three figures the results from the original PANDA-type theory [2] (plots with small squares) display an abrupt increase in the buckling load in the neighborhood of 45 degrees with increasing layup angle, ANG(1). (NOTE: in the multilayer plates angle-ply symmetry, ANG(1)=+θ, ANG(2)=-θ is maintained as the ply angle ANG(1) increases). The jump in buckling load factor in the neighborhood of ANG(1)=45 degrees is caused by the abrupt change in buckling model used in PANDA2, as demonstrated in Fig. 2. For the square plates, for layup angle less than 45 degrees, the panel is physically "long" in the "y" coordinate direction (Fig. 2b), whereas the opposite is true (Fig. 2a) for layup angle greater than 45 degrees. Fig. 2 shows the assumed w-displacement fields used in the original PANDA-type theory [2] for the two models, 2a and 2b.

For the one-layered plate (Fig. 4) the original PANDA-type predictions are too conservative, especially for layup angle ANG(1) less than 45 degrees. For the two-layered plate, $[+\theta, -\theta]_{total}$ (Fig. 5), the original PANDA-type theory is unconservative.

For the four-layered plate, $[+\theta, -\theta, -\theta, +\theta]_{total}$ (Fig. 6), the difference between the original PANDA-type solution and the new alternate solution is less than for the one-layered plate, but the original PANDA-type solution is still unacceptably conservative for layup angle ANG(1) less than 45 degrees, and a large discontinuity exists at the transition from the buckling model pictured in Fig. 2b to that in Fig. 2a.

Except in the case of the one-layered plate, the new alternate solution is slightly conservative when compared to STAGS predictions. The fact that STAGS yields lower predictions than PANDA2 in the neighborhood of ANG(1)=45 degrees in the case of the one-layered plate is unknown at this time. The PANDA2 predictions with the alternate solution are in very good agreement with the predictions of Whitney [8] for the one-layered plate.

Figures 6, 7, and 8 show predictions for four-layered flat plates of increasing aspect ratio, a/b, where "a" is the axial length and "b" is the plate width. There is increasingly good agreement between the original PANDA-type solution [2] and the new alternate solution as the plate aspect ratio a/b increases.

Figures 9 - 12 are analogous to Figures 6 - 8. The applied loading is uniform in-plane shear N_{xy} = 1.0 lb/in rather than axial compression N_x. The new alternate solution in PANDA2 is slightly conservative with respect to the STAGS predictions throughout, mostly because of the aforementioned factor of 0.95 arbitrarily applied to the PANDA2 prediction to compensate for truncation of the trigonometric series expansions for the buckling modal displacement component w. (As with the isotropic flat plate, the in-plane buckling modal displacement components u and v play no role in the analysis of the flat plate with a balanced laminate).

Figure 13 shows the STAGS model used to establish the comparison between STAGS and PANDA2 predictions for one of the points in Fig. 12, that for which the layup angle ANG(1) = 45 degrees.

In the course of the study reported in this section of this paper all STAGS models were automatically generated with use of the PANDA2 processor called STAGSMODEL [24]. The STAGS 480 finite element was always used because this particular finite element includes the t.s.d. effect. The STAGS models are constructed by the PANDA2 processor, STAGSMODEL, in such a way that there are no "induced" prebuckling resultants generated by the Poisson effect, such as the "induced" hoop compression of an axially compressed angle-ply panel that would occur if lateral Poisson expansion of the panel were prevented in the prebuckling phase of the analysis at the axially loaded ends of the panel. The prebuckling resultants are uniform throughout the STAGS models and are equal in value to the applied loads, N_x, N_{xy}, provided by the PANDA2 user.

Cylindrical Panels

Figures 14 - 20 pertain to this section. All results are for four-layered cylindrical panels, $[+45, -45, -45, +45]_{total}$, with total thickness t(total) = 0.04 in. for the four-ply laminate and with material properties: E_{11} = 13.75 msi, E_{22} = 1.03 msi, $G_{12}=G_{13}=G_{23}$=0.420 msi, ν_{minor} = 0.0187273. The panel radius of curvature, r = 6 in. throughout. Figures 14 - 18 are for panels under pure axial compression, N_x = -1.0 lb/in, and Figure 19 is for panels under pure in-plane shear, N_{xy} = 1.0 lb/in. Note that, especially in Figs. 14 and 15, the vertical scale makes the differences among the various predictions appear to be more dramatic than is actually so.

Figures 14 and 15 show predictions for axially compressed cylindrical panels with arc-widths, b = 3 in. and b = 6 in., respectively. In Fig. 14 the predictions from the original PANDA-type theory (legends without the string "0.95*altsol") exhibit the same type of discontinuity shown in Figs. 4 - 7. The discontinuities are caused by the same abrupt change in buckling model discussed previously and demonstrated in Fig. 2. The predictions from the new alternate solution in PANDA2 are conservative (except for one point in Fig. 14 and one point in Fig. 15) with respect to predictions from STAGS.

The plots corresponding to the new alternate solution in PANDA2 with use of the Sanders theory ("SAND" appears in the legend) are somewhat "jumpy". This "jumpiness" results from the strategy used in PANDA2 to obtain converged alternate solutions for panels that are longer in one coordinate direction than the other. The strategy is described in detail in ITEMs 438 and 443 of [15] and briefly in the next section, "Digression....".

Digression: How PANDA2 Searches for Critical Buckling Load Factors

Table 2 lists some results from the computations conducted in SUBROUTINE BUCPAN, where buckling load factors from both the original PANDA-type theory [2] and from the new alternate double-trigonometric-series-expansion theory are obtained. (The original PANDA-type predictions are obtained in SUBROUTINE GENSTB and the new "double-trig" predictions are obtained in SUBROUTINE ALTSOL). The calculations represented in Table 2 correspond to the panel shown in Fig. 16 and to the panel length "a" = 25 in. in Fig. 15. PART 1 of Table 2 lists results from the original PANDA-type of analysis [2]. PART 2 of Table 2 lists results from the new alternate solution. Table 2 and the following explanation are included in this paper because these computations are a very significant part of PANDA2 and the PANDA2 output listed in Table 2, which is an edited version of a portion of the *.OPM file, is new. It is important that PANDA2 users understand what is going on in this crucial part of PANDA2.

PART 1 of Table 2 lists results from the PANDA-type of analysis [2]. The search for the critical (lowest) buckling load factor has become increasingly elaborate over the years since [1] and [2] were published in 1987 because at various times since then comparisons between predictions from PANDA2 and STAGS revealed that PANDA2 had somehow performed an incomplete search and had missed the lowest buckling load and mode shape with respect to m (the number of axial halfwaves), n (the number of circumferential halfwaves) and s (the slope of the buckling nodal lines). The variables, EIGMNC, SLOPEX, MWAVEX, NWAVEX, in Table 2 have the following meanings:

EIGMNC = buckling load factor before any "knockdowns" for transverse shear deformation, imperfections, smeared stringers, etc.

SLOPEX = slope of the buckling nodal lines, s, called "c" or "d" in Eq.(51) of [2], depending on whether the buckling pattern has the form depicted in Fig. 2a or 2b, respectively.

MWAVEX = number of axial halfwaves, m

NWAVEX = number of circumferential halfwaves, n

Seven values of EIGMNC are listed. From left to right these represent the results of searches over the following domains of wavenumbers and buckling nodal line slope, (m,n,s):

1. low values of m; low values of n; entire range of s

2. low values of m; high values of n; entire range of s

3. high values of m; low values of n; entire range of s

4. high values of m; high values of n; entire range of s

5. more extensive search over (m,n) with s = 0.

6. search over (m,n,s) corresponding to possible missed critical values of (m,n)

7. search over (m,0,s) for possible critical "helicoidal" buckling, which is possible especially for axially compressed, laminated composite cylindrical shells.

An illustration of the first four (m,n,s) searches is provided in Fig. 10 on p. 555 of [2] for a complete (360 degrees) axially compressed cylindrical shell. ITEM 443 in [15] provides a better example than the one in this paper because all seven searches lead to different critical buckling load factors and mode shapes, (m,n,s). In the present example, either no searches were conducted or there were no positive eigenvalues for (m,n,s) Domains 4 and 7. That is why the eigenvalue, EIGMNC, has the value 1.00E+17 for those domains. PANDA2 makes decisions on which domains to search depending on panel geometry, loading, and results obtained during searches over previous domains. In this particular example the searches over multiple domains of (m,n,s) reveal only two critical buckling modes, one with m = n = 1 and the other with m = 24 and n = 1. In the example provided in ITEM 443 of [15] all seven domains yielded critical buckling loads with different mode shapes (m(crit), n(crit), s(crit)).

After the seven domains of (m,n,s) are searched, PANDA2 chooses the minimum load factor EIGMNC and corresponding mode shape (m,n,s) as the critical value [in this case 351(1,1,6.39), resembling, by the way, the mode shape shown in Fig. 17, not Fig. 16!]. PANDA2 then refines the search over the range of buckling nodal line slope s for (m(crit), n(crit), s) = (1,1,s) in the neighborhood of the critical value of slope, s = 6.39, previously determined. In this final search, very small increments of slope s are used. The final value of critical buckling load factor and mode shape (m,n,s) from the PANDA-type theory before knockdown to account for transverse shear deformation effects (t.s.d.) is:

EIGVAL(m(crit),n(crit),s(crit)) =347.75(1,1,6.0213)

After knockdown for t.s.d., the final critical buckling load factor from the original PANDA-type theory is 339.32.

PART 2 of Table 2 lists results from the new alternate solution, which is obtained in SUBROUTINE ALTSOL. Initially the upper limits, m_{max} and n_{max}, on numbers of axial and circumferential halfwaves (m,n) in the trigonometric series expansions represented by Eq. (1a,b) is taken to be 5. PANDA2 searches for a minimum critical load with use, in this particular case, of five different sublengths of panel, each sublength one half of the previous sublength, starting with the full length of the panel, 25 inches. In this case the lowest buckling load factor, 397.36, corresponds to a sublength of 3.125 inches. For this critical sublength, 3.125 in., PANDA2 then increases the upper limit on (m,n) from 5 to 7 and recomputes the buckling load factor. The new load factor, 395.88, is knocked down for t.s.d. effects to 384.99 and further knocked down by a factor 0.95 to a value of 365.74 in order to compensate for truncation of the series expansions and incomplete search over sublengths.

In this case (unstiffened panel) the new alternate solution, 365.74, REPLACES the PANDA-type solution, 339.32, because the "high-m" buckling load factor from the PANDA-type analysis, 428.86 (m=24 axial halfwaves), is higher than 365.74. Had the "high-m" buckling load factor been lower than 365.74, it would have been used as the buckling constraint condition rather than the buckling load factor from the new alternate solution.

The remainder of PART 2 of Table 2 lists other knockdown factors which modify the buckling load. In this case of the perfect panel with no stiffeners, all of these factors are unity. The implementation of Arbocz theory [3] into PANDA2 is described in [25]. If the Arbocz theory yields a lower buckling load factor than the original PANDA-type theory, then PANDA2 knocks down the value obtained from the original PANDA-type theory. No such knockdown is used for the new alternate theory because the part of the Arbocz theory used in PANDA2 is based on the assumption of straight buckling nodal lines and is therefore regarded as being more approximate than the new alternate buckling theory in PANDA2.

Back to Numerical Results

In Fig. 15 the STAGS solution and the PANDA2 alternate solution based on Sanders' theory (SAND) both exhibit "valleys" for axial length "a" greater than about 27 in. These "valleys" correspond to a radically different buckling mode from that for the panels with "a" less than about 27 in. Fig. 16 shows the buckling mode from STAGS corresponding to axial length "a" = 25 in., and Fig. 17 shows the mode from STAGS corresponding to axial length "a" = 30 in. In Fig. 15 the "valley" produced by PANDA2 from the new alternate solution has a missing bottom in the range of panel

lengths from about 32 in. to 40 in. That is because in that particular range of panel length "a" the critical number of circumferential halfwaves n in the buckling mode predicted from the original PANDA-type theory [2] is greater than 3, one of the conditions for which PANDA2 overrides the user's wish to employ the new alternate solution. (See Item 3d in the list contained in the subsection entitled "Discussion" above.)

Figure 18 shows the relationship among the various buckling models as functions of panel arc-width "b" for panel length, "a" = 10 in.

Figure 19 is analogous to Figs. 14 and 15, except the loading is now pure in-plane shear, N_{xy} = 1.0 lb/in instead of pure axial compression N_x. Notice that the predictions from the original PANDA-type solution (squares, "right-side-up" triangles) corresponding to the shallowest panels, "b" = 3 in. and "b" = 4 in., each exhibit the familiar discontinuity in behavior. It is caused by the abrupt change in buckling model previously discussed (Fig. 2a vs 2b). There is very good agreement between the STAGS predictions and the predictions from the new alternate solution in PANDA2 for the four different "b"s for which STAGS results were obtained.

Figure 20 displays load-interaction curves from the original PANDA-type theory, the new alternate solution in PANDA2, and STAGS for a particular panel geometry for which there is the largest discrepancy between predictions from the original PANDA-type theory and the new alternate solution in PANDA2. The normalizing factors, N_{xcr}=-344, N_{xycr}=126, are the general buckling loads from the original PANDA-type theory for pure axial compression and pure in-plane shear, respectively. The new alternate theory agrees very well with predictions from STAGS.

NEW "ALTERNATE" GENERAL BUCKLING MODEL FOR CYLINDRICAL PANELS WITH RINGS AND STRINGERS TREATED AS DISCRETE BEAMS

Introduction

After completion of the modifications described in the previous section but before the modifications described in this and the next major section, the writer optimized a ring and stringer stiffened composite cylindrical shell with the following properties and loading:

Length and radius of cylindrical shell, L = 60 in., r = 6.0 in. With PANDA2 the cylindrical shell is analyzed as a panel that spans 180 degrees. Results for such a panel, simply supported along the two generators, are identical to predictions for a complete (360-degree) cylindrical shell. Boundary conditions: both ends simply supported. Imperfections: None. The shell is assumed to be perfect.

Skin of cylindrical shell has four layers, [+θ, -θ, -θ, +θ]; Ply properties: moduli E_{11} = 13.75 msi, E_{22} = 1.03 msi, $G_{12} = G_{13} = G_{23}$ = 0.42 msi, ν_{minor} = 0.01873, weight density = 0.057 lb/in**3; allowable maximum stresses set very high to avoid active stress constraints.

Internal rings and external stringers of rectangular cross section; Stiffener properties: Entire cross section with layup angle = 0 with respect to the axis of the stiffener; Stiffener material: E_{11} = 14.0 msi, E_{22} = 1.04 msi, $G_{12} = G_{13} = G_{23}$ = 0.40 msi, ν_{minor} = 0.018, weight density = 0.06 lb/in**3; allowable maximum stresses set very high to avoid active stress constraints.

The stiffened composite cylindrical shell was optimized for the following two load sets:

Load Set 1: Uniform axial compression, N_x = -700 lb/in, Uniform in-plane shear (torque), N_{xy} = + 40 lb/in

Load Set 2: Uniform axial compression, N_x = -100 lb/in, Uniform in-plane shear (torque), N_{xy} = +150 lb/in

All factors of safety for stress and buckling are set equal to unity. The decision variables and lower and upper bounds during optimization are:

T(1) = thickness of the first ply of the cylindrical skin; (0.005 < T(1) < 0.03 in.)

ANG(1) = layup angle of 1st ply; (20<ANG(1)<70 deg)

H(STR) = height of stringers;(0.10 < H(RNG) < 1.0 in.)

T(3) = thickness of the stringers; (0.03 < T(3) < 0.2 in.)

H(RNG) = height of rings; (0.10 < H(RNG) < 1.0 in.)

T(4) = thickness of rings; (0.02 < T(4) < 0.2 in.)

B(STR) = stringer spacing; (3.77 < B(STR) < 6.28 in.)

B(RNG) = ring spacing; (6.0 < B(RNG) < 12.0 in.)

The thickness of the second ply of the cylindrical skin, T(2), is linked to the thickness of the first ply, T(2) = T(1), and the layup angle of the second ply of the cylindrical skin, ANG(2), is linked to the layup angle of the first ply, ANG(2) = -1.0*ANG(1).

Starting values of the decision variables:

B(STR) = 6.00 in., H(STR) = 0.500 in., T(1) = T(2) = 0.0100 in.; ANG(1) = -ANG(2) = 45.0 degrees, T(3) = 0.0500 in., B(RNG) = 10.0 in.; H(RNG) = 0.500 in., T(4) = 0.05 in.

After optimization via SUPEROPT [25] with the "alternate solution" switch turned ON, but BEFORE the modifications to PANDA2 described in this and the next major section, PANDA2 obtained the following optimum design:

B(STR) = 3.7699 in., H(STR) = 0.1237 in., T(1) = T(2) = 0.008099 in.; ANG(1) = -ANG(2) = 69.3 degrees, T(3) = 0.12584 in., B(RNG) = 6.0 in.; H(RNG) = 0.21999 in., T(4) = 0.02 in.

An elaborate STAGS model of the complete (360-degree) ring and stringer stiffened cylindrical shell optimized by PANDA2 was constructed (not with the processor STAGSMODEL because STAGSMODEL will not at present handle cases that include rings). Input data for STAGS (the *.bin and *.inp files) are listed in Table 444.2 of [15]. The 410 finite element was used in the STAGS model because the 480 finite element is presently not available for use with rings and stringers treated as discrete "beams". (There is no "280" finite element in the STAGS library of finite elements as if this writing). Hence, the STAGS model does not include the t.s.d. effect, which, according to PANDA2, is small in this case.

For the optimum design listed above, STAGS obtained a critical buckling load factor, P(crit) = 0.77519, considerably lower than the factor very close to 1.0 obtained by the version of PANDA2 that existed at the time that STAGS run was made. PANDA2's analysis was therefore significantly unconservative. The buckling mode from STAGS corresponding to this unfeasible "optimum" design, displayed in Fig. 21, has many waves along the axis and around the circumference. It corresponds to a type of general instability because the rings and stringers undergo significant deflection in the buckling mode.

It is clear from an inspection of the buckling mode shown in Fig. 21 that a general instability model in which stringers and rings are "smeared out" (averaged) may well be unacceptably unconservative. Therefore, a decision was made to include a new buckling model in PANDA2: a model in which both rings and stringers are treated as discrete in the analysis of general instability. The capability of the new "alternate solution" branch was expanded in order to incorporate this new buckling model. into PANDA2.

Theory

1. The new buckling model for general instability of cylindrical panels is based on the same double trigonometric series expansions listed as Eqs (1a,b) in the previous major section.

2. The strain energy of a stiffener is given by:

$$U = \frac{1}{2}\int_x \int_y \mathbf{e}^T \mathbf{G} \mathbf{e}\, dydx \tag{17}$$

in which **G** is given by,

$$\mathbf{G} = \begin{bmatrix} EA & 0 & 0 & 0 \\ 0 & EI_x & 0 & 0 \\ 0 & 0 & EI_y & 0 \\ 0 & 0 & 0 & GJ \end{bmatrix} \tag{18}$$

where EA is the axial stiffness of the stiffener, EI_x is the bending stiffness of the stiffener with use of the stiffener axis of centroids as a reference (bending in a plane normal to the plane of the panel skin), EI_y is the bending stiffness of the stiffener in a plane parallel to the plane of the panel skin at the stiffener attachment, and GJ is the torsional rigidity of the stiffener. The strain energy associated with non-zero polar moment of inertia, I_{xy}, of the stiffener cross section is ignored. For the contribution of each STRINGER to the strain energy and work done by prebuckling loads during buckling modal displacements, only the integration over the axial length x is performed; for the

contribution of each RING only the integration over the circumferential arc length y is performed.

3. The strain vector, **e**, (centroidal axis) is given by

$$\mathbf{e} = \begin{bmatrix} e_1 & k_1 & k_2 & k_{12} \end{bmatrix} \tag{19}$$

in which e_1 is the axial strain, k_1 is the change in curvature in the plane normal to the panel skin at the attachment point of the stiffener to the skin, k_2 is the change in curvature in the plane parallel to the panel skin at the attachment point of the stiffener to the skin, and k_{12} is the twisting of the stiffener.

For stringers:

$$\begin{aligned} e_1 &= u_{,x} - w_{,xx}\, e_{str} \\ k_1 &= -w_{,xx} \\ k_2 &= v_{,xx} - w_{,yxx}\, e_{str} \\ k_{12} &= w_{,xy} \quad \text{(shallow shell theory)} \end{aligned} \tag{20}$$

For rings shallow shell theory is used:

$$\begin{aligned} e_1 &= v_{,y} + w/r - w_{,yy}\, e_{ring} \\ k_1 &= -w_{,yy} \\ k_2 &= u_{,yy} - w_{,xyy}\, e_{ring} \\ k_{12} &= w_{,xy} \end{aligned} \tag{21}$$

in which e_{str} is the distance from the stringer shear center to the reference surface of the panel skin, positive for external stringers, and e_{ring} is the distance from the ring shear center to the reference surface of the panel skin, positive for external rings. A term, $-w_{,x}/r$, is neglected in the expression for k_2 for the rings. It is felt that in cases for which there is a significant difference between the buckling load predicted from a model in which the stiffeners are smeared vs that predicted from a model in which the stiffeners are discrete, the critical repeating buckling pattern will span a shallow portion of the panel, as is the case in the example shown in Fig. 21.

Shallow shell theory is used here because discrete stiffener theory is needed only if the wavelength of the critical buckling pattern is of the same order as the stiffener spacing. It is assumed that the stiffener spacing is close enough so that the section of panel bounded by adjacent stiffeners is a shallow shell.

4. The work done by the prebuckling forces in the web (F_1) and outstanding flange (F_2) of a stiffener during buckling modal displacements:is given by:

$$W = \frac{1}{2} \sum_{web(i=1)}^{flange(i=2)} F_i \int_L \left(r_x^2 + r_y^2 \right) dL \tag{22}$$

in which, for stringers:

$$r_x = w_{,x} \qquad r_y = v_{,x} - w_{,yx}\, z(i) \tag{23a}$$

and for rings:

$$r_x = w_{,y} \qquad r_y = u_{,y} - w_{,xy}\, z(i) \tag{23b}$$

where $z(i)$ is the distance from the panel skin reference surface to the centroid of the ith stringer segment or ith ring segment. (For example, i = 1 = web and i = 2 = outstanding flange). The quantity, L, is the length of stiffener axis over which the integration is performed.

Discussion

The following points are emphasized:

1. The alternate solution for general instability is performed only for SUBCASE 1, which corresponds to conditions midway between rings, except that in this particular application the hoop preload in the panel skin is averaged over the distance between adjacent rings, whereas in the original PANDA-type solution the value of the hoop preload in the panel skin at the midbay location is used.

2. Whether or not discrete stiffeners are to be included in a buckling model depends not only on the user-provided "alternate solution switch", IALTSN, but also on an internal PANDA2 index, IDISCT: 0 means NO; 1 means YES. The index IDISCT is generated by PANDA2, not by the PANDA2 user. Whether IDISCT is set by PANDA2 to be zero or unity depends on considerations analogous to those listed as Items 3a - 3f in the previous subsection entitled "Discussion", but applied to a subdomain of the entire panel, as described in Item 5 below.

3. The new discrete stiffener model is used only for cylindrical panels.

4. Discrete stiffeners are included only for blades or tees or jays or zees, and not for isogrid-stiffened panels nor for panels with hat stiffeners or for the truss-core

sandwich configuration.

5. A subdomain of the complete panel of width and length equal to at most THREE stiffener spacings in each coordinate direction is included in the model of general buckling with discrete stiffeners. An example of such a subdomain of a shell similar to that depicted in Fig. 21 is shown in Fig. 22.

6. As with the alternate solution for local buckling described in the previous major section of this paper, the upper limits, m_{max} and n_{max}, on the number of axial halfwaves m and hoop halfwaves n used in the double trigonometric series expansions, Eqs. (1), is seven.

7. If discrete stiffeners are to be included in the general buckling model (IALTSN=1 and IDISCT=1) then the proper wall stiffnesses (C_{ij}) and in-plane loads (N_x, N_y, N_{xy}, N_{x0}, N_{y0}) must be used for the panel skin portion of the structure, and the proper preloads in the discrete stiffeners must be used for the stringers and rings. This is taken care of automatically by PANDA2.

8. The alternate solution (double-trigonometric series expansion) is used for BOTH the current design (IDESGN=0) and each design perturbation (IDESGN=1). The buckling load factor corresponding to each design perturbation is computed with use of the Rayleigh quotient, as described in Item 5 in the subsection entitled "Discussion" in the previous major section. (see Eq. (15)).

9. Unlike the strategy described in the previous major section for the alternate solution for unstiffened panels or an unstiffened portion of a stiffened panel, in which the buckling margin from the alternate solution REPLACES that corresponding to the PANDA-type solution [2] for the same type of buckling (see Table 2), in the case of the new alternate solution with discrete stiffeners, BOTH the old PANDA-type "smeared" stiffener general buckling margin [2] AND the new "alternate solution" margin are RETAINED.

10. A "knockdown" factor of 0.85 is applied to the alternate general buckling load factor in order to compensate for truncation of the double trigonometric series expansions at seven halfwaves in each coordinate direction and to compensate for the use of a subdomain. The factor of 0.85 was arrived at as a result of many comparisons between PANDA2 and STAGS during the development of the new alternate buckling solution for general instability.

Why does PANDA2 use a subdomain?

The critical buckling mode obtained by STAGS for the complete cylindrical shell displayed in Fig. 21 has axial and hoop half-wavelengths approximately equal to the ring and stringer spacings, respectively. Since there are ten rings and ten stringers in the complete cylindrical shell shown in Fig. 21, this very complicated buckling mode shape cannot accurately be predicted directly by PANDA2 with use of the alternate theory, for which the maximum number of axial and hoop halfwaves over the structural domain is equal to seven, as just described in Item 6 above. Therefore, the model for general buckling with discrete rings and stringers usually represents a subdomain of the complete shell.

In particular, a domain containing at most four rings and four stringers is included in the "alternate" general buckling model (three stiffener spacings in each coordinate direction). Two of the four discrete stringers run along the two longitudinal edges of the new, smaller structural domain, and two of the four discrete rings run along the two curved edges of the new, smaller structural domain. Each of these "edge" stiffeners is given half the stiffness of each corresponding internal stiffener, and simple support (antisymmetry) conditions are imposed on the four edges of the subdomain. An example of such a subdomain is shown in Fig. 22. (Figure 22 shows a STAGS model, not a PANDA2 model. There is no two dimensional finite element model in PANDA2).

The logic behind this strategy of selecting a subdomain for analysis by double trigonometric series expansions is as follows:

1. In a case for which the buckling load factor from a model in which the stiffeners are treated as discrete is significantly lower than that from a model in which the stiffeners are "smeared" (such as shown in Fig. 21), the dominant axial and circumferential wavelengths in the critical buckling pattern are likely to be similar to the corresponding stiffener spacings. Since this buckling pattern repeats many times over the entire structure, it is sufficient to use a subdomain that is large enough to capture only a few halfwaves in each coordinate direction in order to obtain a reasonably accurate prediction of general buckling of the entire panel, especially when one is involved in the PRELIMINARY design phase of a project, for which PANDA2 is intended.

2. There will be many cases (in fact, probably most

cases) for which the "smeared stiffener" model [2] is a good one. The new alternate solution with discrete stiffeners, covering possibly a rather small subregion (especially if the stiffener spacings are small), will in these cases probably significantly overestimate the general buckling load. That is why margins from BOTH the original PANDA-type "smeared stiffener" ("global") model [2] and the new alternate (subdomain) solution with discrete stiffeners must be retained in the PANDA2 model. If the new alternate subdomain model yields a very high buckling load factor because the subdomain is too restrictive, then that artificially high buckling load factor will naturally be ignored during the design process because that particular behavioral constraint will not be active. The general buckling load factor from the original "smeared stiffener" model [2] is still retained by PANDA2, and that model includes the entire panel, not just a subdomain of it. If a long wavelength general buckling mode is critical, then the "smeared stiffener" model will capture it with reasonably good accuracy. An example is shown later.

One might wonder, should not there be two new "alternate-solutions-with- discrete-stiffeners" for a cylindrical panel stiffened by both rings and stringers: one solution in which both rings and stringers are treated as discrete and another for just the region between two adjacent rings in which only the stringers are treated as discrete? As of this writing it is felt that it is unnecessary to include a special "between-adjacent-rings" alternate model. It is felt that the subregion model in which both rings and stringers are treated as discrete will automatically cover the inter-ring region with only stringers smeared out.

Numerical Results

The same ring and stringer stiffened composite cylindrical shell described in the subsection entitled "Introduction" was reoptimized after the modifications to PANDA2 described in this major section were implemented. (The new discretized "skin"-ring module capability to be described in the next major section had also been incorporated into PANDA2 when this run was made).

All conditions were the same as before except that the lower bounds of ring thickness T(4), stringer spacing B(STR), and ring spacing B(RNG) were changed as follows:

T(4) = thickness of the rings; (0.03 < T(4) < 0.2 in.)

B(STR) = stringer spacing; (1.885 < B(STR) < 6.28 in.)

B(RNG) = ring spacing; (3.0 < B(RNG) < 12.0 in.)

Figure 23 shows the objective (panel weight) plotted vs design iterations for a 2nd SUPEROPT [25] run. During a typical SUPEROPT execution a panel is automatically reoptimized many times from different starting designs, each starting design generated via a random process described in [25]. In this particular case there are eight reoptimizations starting from the designs represented by spikes in the plot in Fig. 23. Notice that in the various reoptimizations the design converges to local minimum weights that are different from eachother. The purpose of SUPEROPT is to search for a GLOBAL minimum weight design. PANDA2 chooses the "best" design among those processed during the entire SUPEROPT run. Note that in general this will not, of course, be the last design processed. By "best" is meant the least weight design that PANDA2 determines is either "FEASIBLE" or "ALMOST FEASIBLE". By "FEASIBLE" is meant a design for which there is no margin with a value less than -0.01; By "ALMOST FEASIBLE" is meant a design for which there is no margin with a value less than -0.05.

Figures 24 and 25 show the evolution of some of the design margins during the SUPEROPT run. (Only those margins corresponding to load SUBCASE 1, conditions midway between adjacent rings, called "midbay" in the plots, are displayed in this paper in order to save space; similar plots exist corresponding to load SUBCASE 2, conditions at the ring locations.) Figure 24 corresponds to margins generated for Load Set 1: N_x = -700 lb/in and N_{xy} = +40 lb/in. Figure 25 corresponds to margins generated for Load Set 2: N_x = -100 lb/in and N_{xy} = +150 lb/in.

The "best" design encountered during the approximately 271 design iterations during the SUPEROPT run has the dimensions:

B(STR) = 1.885 in., H(STR) = 0.14068 in., T(1) = T(2) = 0.0062797 in., ANG(1) = -ANG(2) = 70.0 degrees, T(3) = 0.081042 in., B(RNG) = 4.1992 in., H(RNG) = 0.12947 in., T(4) = 0.03 in.

The weight of 180 degrees of the 60-inch long stiffened cyl. shell = 2.092 lbs.

Table 3 lists the design margins computed by PANDA2 corresponding to the optimum design. None of the

stress margins is close to being critical because the allowable stresses were set very, very high in order to make sure that buckling governs the evolution of the design.

For Load Set 1, SUBCASE 1 (midway between rings) the following margins are critical or fairly close to being critical:

9 7.70E-02 buck.(SAND);simp-support local buck.; (0.95*altsol);FS=1.0

11 1.25E-01 buck.(SAND);simp-support general buck; M=1;N=2;slope=100.;FS=0.999

12 6.66E-04 buck.(SAND);simp-support general buck; (0.85*altsol);FS=0.999

13 2.45E-01 buck.(SAND);rolling with local buck.; M=2;N=1;slope=0.09;FS=1.

For Load Set 1, SUBCASE 2 (at rings) the following margins are critical or fairly close to being critical:

9 3.34E-06 buckling margin stringer Iseg.3 . Local halfwaves=1 .RNGS;FS=1.0

10 3.28E-03 buck.(SAND);simp-support local buck.; (0.95*altsol);FS=1.0

12 9.89E-03 buck.(SAND);rolling with local buck.; M=1;N=1;slope=0.3095;FS=1.

For Load Set 2, SUBCASE 1 (midway between rings) the following margins are critical or fairly close to being critical:

10 4.00E-04 buck.(SAND);simp-support local buck.; (0.95*altsol);FS=1.0

12 2.25E-04 buck.(SAND);simp-support general buck; M=1;N=3;slope=7.7273;FS=0.999

13 2.30E-01 buck.(SAND);simp-support general buck; (0.85*altsol);FS=0.999

14 6.62E-02 buck.(SAND);rolling with local buck.; M=5;N=1;slope=0.9856;FS=1.0

For Load Set 2, SUBCASE 2 (at rings) the following margins are critical or fairly close to being critical:

11 -1.24E-02 buck.(SAND);simp-support local buck.; (0.95*altsol);FS=1.0

13 5.02E-02 buck.(SAND);rolling with local buck.; M=5;N=1;slope=0.9856;FS=1.0

Two STAGS models of the optimized shell were set up, both containing the full 360 degrees of the cylindrical shell. In the first STAGS model only six ring spacings were included, corresponding to a sublength of the cylindrical shell of 6 x 4.1992 = 25.1958 in. The sublength was used to avoid very long STAGS runs on the computer. A fine mesh is required in order to capture local buckling between adjacent stringers and rings.

Figures 26 and 27 display the critical buckling modes from STAGS for Load Set 1 and Load Set 2, respectively, for the STAGS model with cylinder sublength = 25.1958 in. The buckling load factors from STAGS are 1.0304 for Load Set 1 and 1.1326 for Load Set 2. Both of these critical load factors correspond to a form of general instability with many waves in both coordinate directions, just the type of buckling that the new alternate solution for general instability with discrete stiffeners is intended to capture with reasonable accuracy.

The STAGS buckling load factor for Load Set 1, 1.0304, is very close to the prediction of PANDA2 for general instability from the new alternate model, 1.000666 [NOTE: buckling load factor = (factor of safety)*(margin + 1); factor of safety = 1.0; Margin No. 12 for Load Set 1, SUBCASE 1 = 0.000666, hence buckling load factor = 1.0*(0.000666 + 1.0) = 1.000666].

For Load Set 2 the STAGS prediction, 1.1326, is somewhat below the buckling load factor from PANDA2 obtained from the new alternate solution, 1.230 (see Margin No. 13, Load Case 2, SUBCASE 1: 0.230), and above the buckling load factor from PANDA2 obtained from the original PANDA-type solution, 1.000225 (see Margin No. 12, Load Case 2, SUBCASE 1: 0.000225). The sublength STAGS model (the six-ring-spacing model shown in Fig. 27) is insufficiently long to capture the general buckling mode predicted by PANDA2 from the original PANDA-type solution [2] because this PANDA2 model predicts buckling with only one half wave in the axial coordinate direction (m = 1; see Margin No. 12, Load Case 2, SUBCASE 1).

Figure 28 shows results from a STAGS model for the full 60-inch length of the cylindrical shell. This full-length model is used only for Load Set 2, N_x = -100 lb/in and N_{xy} = +150 lb/in. The buckling mode predicted by STAGS is the same as that predicted by the original PANDA-type model [2] in PANDA2: m = 1 axial halfwave, n = 3 circumferential waves as listed for Margin No. 12, Load Set 2, SUBCASE 1. The buckling load factor from STAGS, 0.94698, is about five per cent lower than that predicted by PANDA2, 1.000225. Hence, it appears that in this case PANDA2's two predictions of general instability, one from the original PANDA-type theory, 1.000225, and the other from the new alternate solution, 1.230, are slightly unconservative. This small degree of unconservativeness can easily be compensated by use of a factor of safety for general instability that is larger than unity. It is felt that it does not seriously compromise PANDA2's qualification as a tool for the preliminary design of stiffened panels and shells.

A question arises, why did the STAGS sublength model for Load Set 2 (Fig. 27) not capture the LOCAL instability predicted by PANDA2 to occur at a load factor very close to unity for both SUBCASEs 1 and 2? One of the reasons is that the PANDA2 local buckling load factors from the new alternate solution, 1.0004 (see Margin No. 10, Load Set 2, SUBCASE 1) and 0.9876 (see Margin No. 11, Load Set 2, SUBCASE 2, are derived with neglect of the effect of possible elastic restraint of the stiffeners during the transition from prebuckling to buckling states. As mentioned previously, the new alternate LOCAL buckling analysis is based on the assumption that the portion of panel between adjacent stiffeners is simply supported and the stiffeners are absent (except that they capture their share of the applied loading, of course). Also, the alternate solution for local buckling is "knocked down" by the factor 0.95 in PANDA2 and t.s.d. is neglected in the STAGS model, which, because of the presence of discrete beams, is constructed with 410 finitie elements rather than with 480 finite elements.

The ring and stringer stiffened composite cylindrical shell was reoptimized with the alternate solution switch, IALTSN, turned OFF, that is, IALTSN = 0. This saves computer time but may well lead to unconservative "optimum" designs. Again, the PANDA2 processor SUPEROPT was used for the optimization.

The "best" design encountered during the approximately 271 design iterations during the SUPEROPT run has the dimensions:

B(STR) = 1.885 in., H(STR) = 0.14092 in., T(1) = T(2) = 0.0056963 in., ANG(1) = -ANG(2) = 70.0 degrees, T(3) = 0.082716 in., B(RNG) = 4.9810 in., H(RNG) = 0.14150 in., T(4) = 0.03 in.,

The weight of 180 degrees of the 60-inch long stiffened cyl. shell = 1.946 lbs. (Compare with 2.092 lbs.)

Figure 29 shows the critical buckling mode from Load Set 1 predicted by STAGS for this new optimum design obtained by PANDA2. The critical buckling load factor from STAGS is 0.83716, and the critical buckling mode is again general instability with many waves. Note that although the optimum weight of the reoptimized shell (1.946 lbs) is only seven per cent less than that obtained (2.092 lbs) with the alternate solution switch, IALTSN, turned ON, the buckling load factor, 0.837, is about 19 per cent less than that obtained with IALTSN = 1: 1.0304 (Fig. 26). With the alternate solution turned OFF, PANDA2 generates not only an unfeasible design according to STAGS, but a design that is less efficient.

NEW "SKIN"-RING DISCRETIZED SINGLE-MODULE MODEL FOR INTER-RING BUCKLING OF CYLINDRICAL PANELS

Introduction

Until now the only prebuckling/buckling models in PANDA2 that involved discretized (BOSOR4-type [28]) models of the panel or parts of the panel were the following:

1. Single skin-stringer discretized module such as that shown in Fig. 1. This skin-stringer discretized model is used for local buckling and local postbuckling between stringers and rings (Fig. 1b), for wide-column buckling between rings (Fig. 22c, p. 526 of [1]), and for local, approximately prismatic, transverse bending ("pillowing" under normal pressure) between stringers and rings (Fig. 56, p. 555 of [1]). This "single skin-stringer module" model includes a width b(stringer) of panel equal to a single stringer spacing. The model contains one stringer cross section plus the panel skin of width b(stringer) to which the stringer is attached (width b(stringer)/2 on each side of the web root of the stringer). It is assumed that the behavior predicted with this "single-module" model repeats approximately k times across with panel width, in which k is the number of stringers in the panel.

2. Entire panel width with smeared stringers and rings. This model is used for global prebuckling deflection under pressure (Fig. 55, p. 554 of [1]) and for overall buckling of a panel in which the axial load, N_x, varies across the width of the panel.

3. Entire panel width with discrete stringers (Fig. 36, p. 539 of [1]). Actually, this model is NOT used by PANDA2 but is produced via the PANDA2 processor called "PANEL" after optimization by PANDA2. This discretized model is used as an input file for BOSOR4 [28] for a panel previously optimized by PANDA2.

In particular, there has been no PANDA2 model in which the segments of a RING are discretized. Until now the RINGs have been treated as "second class citizens": they have been either represented as simple support conditions, or they have been smeared out (averaged), or they have been treated as discrete beam-columns with undeformable cross section (previous section in this paper).

New "skin"-ring single discretized module model

Now there exists in PANDA2 a discretized "skin"-ring module model analogous to the discretized skin-stringer module model. The single "skin"-ring module model includes one ring cross section plus an axial length of panel equal to the ring spacing, b(ring) (b(ring)/2 on each side of the root of the web of the ring). The word "skin" is enclosed in quotation marks in the term, "skin"-ring module, because it is not just the "skin" that is included, but the skin with smeared stringers, if there are any stringers. The new discretized "skin"-ring module is used for buckling analysis under the following circumstances:

1. The panel is cylindrical.

2. The rings are either blades, tees, jays, or zees, or no rings.

3. The inter-ring buckling mode from the PANDA-type closed form solution has at most three axial half waves between rings.

4. The Jones-Heinneman-Almroth prebuckling solution [20] is obtained in SUBROUTINE SKIN. (Under certain conditions this prebuckling analysis is skipped).

5. Either the applied axial load, N_x, or the applied hoop load, N_y must be less than zero.

6. The in-plane shear load, N_{xy}, must satisfy:
$N_{xy} \le 2\sqrt{N_x^2 + N_y^2}$.

The discretization in the "skin"-ring single module model is the same as it is for the skin-stringer module (Fig. 1a), that is, there are 11 nodal points in each segment of the single "skin"-ring module. The segment numbering is the same as that for the skin-stringer module.

Implementation of the new "Skin"-Ring Discretized Module Model in PANDA2

In order to implement this new model in PANDA2, it was necessary to modify most of the PANDA2 source libraries. New versions of SETUP and GLOBST were required (called SETUP2 and GLBST2). These new processors generate "template" stiffness/load-geometric matrices (SETUP2) for the "skin"-ring discretized module and fill appropriate labelled common blocks (GLBST2). It was necessary to write new subroutines, ARRYS2 and STABL2, analogous to ARRAYS and STABIL, through which the governing simultaneous, linear, homogeneous algebraic equations, $\mathbf{Ax} = \lambda \mathbf{Bx}$, for bifurcation buckling of the discretized "skin"-ring module are generated. These equations are different from those for the skin-stringer discretized module because the "skin"-ring module is cylindrical, whereas the skin-stringer module is prismatic. The equations for the "skin"-ring discretized module are the same as those used in the BOSOR4 program [28]. Therefore, certain subroutines called by SUBROUTINE STABIL in BOSOR4 could be used directly for the implementation in PANDA2. These "BOSOR4" subroutines are now called by SUBROUTINE STABL2, which is called by SUBROUTINE ARRYS2. The new SUBROUTINE ARRYS2 is called by SUBROUTINE BUCKLE. The "skin"-ring module equations are derived in SUBROUTINE BUCKLE whenever SUBROUTINE BUCKLE is called with the index, IGLOB = 2, in its argument list. A long segment of coding had to be added to SUBROUTINE STRUCT to generate the new buckling load factors corresponding to the several different types of buckling that are possible with the "skin"-ring module.

Typical Buckling Behavior of a "skin"-Ring Module

The buckling behavior of a "skin"-ring module can be quite complicated, as demonstrated in Fig. 8 on p. 1287 of [26], reproduced here as Fig. 30. In Fig. 30 there are three rows of module images. In these three rows of

module images four different buckling modes can be characterized:

1. A mode dominated by sidesway of the ring web and outstanding flange. (Fig. 30, top row, leftmost image, for example). The panel "skin" participates little if at all. This mode usually has a small number of circumferential waves.

2. A mode dominated by the "skin" buckling, with symmetry conditions governing midway between adjacent rings, that is, at the top and bottom of the module model. (Fig. 30, top row, rightmost image, for example). This mode usually has an intermediate number of circumferential waves.

3. A mode dominated by buckling of the ring web. (Fig. 30, second row, rightmost image, for example). This mode usually has a large number of circumferential waves.

4. A mode in which the ring cross section does not deform. The entire module undergoes a translation with some deformation of the panel skin. (Fig. 30, the three leftmost images in the third row, for example). This mode is analogous to the skin-stringer module buckling mode called "wide column buckling", shown in Fig. 22c on p. 526 of [1], for example. While it is permitted in PANDA2's discretized skin-stringer module model, this mode is NOT permitted in the new PANDA2 "skin"-ring model. in the "skin"-ring model the ring web root is prevented from displacing normal to the shell surface in the bifurcation buckling phase of the analysis.

In the new implementation of the discretized "skin"-ring module in PANDA2, the first three modes are permitted but the fourth, which would represent global buckling of a cylindrical panel of infinite length, is not permitted because it might lead to overly conservative predictions of general buckling and hence optimized designs that are too heavy. This "general" buckling mode is prevented in the discretized single "skin"-ring module model by forcing the normal buckling modal displacement w of the panel skin at the ring web root to be zero. A "general" buckling load factor derived from the discretized "skin"-ring module is not needed by PANDA2 because general buckling is already covered by two other models: a PANDA-type (closed form) model in which the stiffeners are smeared out [2] and the new alternate model in which the stiffeners are treated as discrete beam-columns, as described in the previous major section.

Strategy

Because the buckling of the discretized "skin"-ring module can have three different critical modes with respect to the number of circumferential halfwaves n, the following strategy is used in this new part of PANDA2:

1. The search for the critical number, n(crit), of circumferential halfwaves n is begun at the critical value of n obtained for inter-ring buckling from the simple PANDA-type model [2].

2. PANDA2 searches for a minimum buckling load factor as a function of number of circumferential halfwaves n. When it finds a minimum load factor vs. n, it determines the buckling mode corresponding to n(crit).

3. Depending on the characteristics of the buckling mode shape determined from a scan of the critical eigenvector, PANDA2 sets up a buckling margin phrase with one of the following strings:

"Inter-ring buckling" (maximum normal buckling modal displacement w is somewhere in the cylindrical skin), or

"Ring web buckling" (maximum normal buckling modal displacement w is in the ring web but not at the outstanding tip of the ring web), or

"Ring sidesway" (maximum normal buckling modal displacement w is at the tip of the ring web).

4. PANDA2 next explores a "high-n" range to ascertain if there is another minimum buckling load factor with respect to n in this range. The "high-n" search starts at a circumferential wavenumber n one increment higher than the highest n covered by the search in Item 2. The highest n to be included in the "high-n" search is three times the highest n covered by the search in Item 2. If buckling load factors are decreasing with increasing n at this upper limit of n, PANDA2 keeps computing buckling load factors for increasing n until it detects a minimum load factor with respect to n.

5. If a new minimum buckling load factor vs. n is detected by PANDA2, then PANDA2 computes the mode shape and scans it as in Item 3, assigning the proper margin phrase to the new buckling constraint. In this case one of the strings, "Inter-ring buckling" or

"Ring web buckling" or "Ring sidesway" is preceeded by the string, "Hi-n".

6. PANDA2 next explores the "low-n" range to ascertain if there is yet another minimum buckling load factor with respect to n in this range. The "low-n" search starts at n = 1 and ends just below the lowest n explored in the search described in Item 2.

7. If a new minimum buckling load factor vs. n is detected by PANDA2, then PANDA2 computes the mode shape and scans it as in Items 3 and 5, assigning the proper margin phrase to the new buckling constraint. In this case one of the strings, "Inter-ring buckling" or "Ring web buckling" or "Ring sidesway" is preceeded by the string, "Lo-n".

More strategy

During the multiple explorations over circumferential wavenumber n just described, PANDA2 generally covers a very wide range of n. This wide range of n usually includes values of n that correspond to critical values for buckling of the various segments of the ring as determined from the simple PANDA-type theory [2] and, of course, the values of n corresponding to inter-ring buckling as determined from the simple PANDA-type theory.

PANDA2 performs the PANDA-type buckling computations for the ring segments and for the panel skin between rings AFTER it has already obtained the buckling loads from the new discretized "skin"-ring module model. Therefore, it knows whether or not to ignore the results from the less sophisticated PANDA-type models [2] because they have been superseded by the more rigorous evaluation represented by the discretized "skin"-ring module model.

PANDA2 tells the user what is going on in this respect. With use of the NPRINT = 2 output option in MAINSETUP (*.OPT file), PANDA2 writes to the *.OPM file information such as that listed in Table 4. Analogous output is listed for other types of buckling computed from the simple PANDA-type theory for stiffener segments in SUBROUTINE STFEIG and for the panel skin in SUBROUTINE BUCPAN.

Numerical Results

The new discretized "skin"-ring module capability in PANDA2 was tested by optimizing via SUPEROPT [25] an isotropic internally T-ring stiffened aluminum cylindrical shell subjected to uniform external hydrostatic pressure. The dimensions, material properties, boundary conditions, loading, decision variables and their lower and upper bounds and starting values are as follows:

Length and radius of cylindrical shell, L = 500 in., r = 100 in. As described in the previous major section, in PANDA2 the complete (360 degrees) cylindrical shell is analyzed as a panel that spans 180 degrees. Boundary conditions: both ends simply supported; Imperfections: None. The shell is assumed to be perfect. Skin of cylindrical shell has one isotropic layer. Internal rings with T-shaped cross section. No faying flange [B2(RNG)=0]. Material: Isotropic, modulus E = 10 msi, ν = 0.3, density = 0.1 lb/in**3. Allowable maximum stresses: set very high to avoid active stress constraints.

The ring stiffened cylindrical shell was optimized for the following single load set:

Uniform axial compression, N_x = -10000 lb/in; Uniform hoop compression, N_y = -20000 lb/in; Uniform pressure, p = -200 psi

All factors of safety for stress and buckling are set equal to unity.

The decision variables and lower and upper bounds during optimization are:

T(1) = thickness of skin; (0.05 < T(1) < 3.00 in.)

B(RNG) = ring spacing; (10.0 < B(RNG) < 30.0 in.)

H(RNG) = height of rings; (0.50 < H(RNG) < 10. in.)

W(RNG) = width of flange; (0.50 < W(RNG) < 10. in.)

T(2) = thickness of ring web; (0.05 < T(2) < 2.00 in.)

T(3) = thickness of ring flange; (0.05 < T(4) < 2.0 in.)

Starting values of the decision variables:

T(1) = 0.250 in., B(RNG) = 20.00 in., H(RNG) = 5.00 in., W(RNG) = 5.00 in., T(2) = 1.00 in., T(3) = 1.00 in.

The cylindrical shell was optimized via a SUPEROPT run. During optimization the "alternate buckling

solution switch", IALTSN, was turned OFF (IALTSN = 0).

Figure 31, analogous to Fig. 23, shows the "panel" weight vs design iteration number resulting from the SUPEROPT run. In this case there were 12 automated re-optimizations starting from different randomly selected designs represented by the spikes in the plot in Fig. 31. (The 12th re-optimization is incomplete). The evolution of the margins corresponding to conditions midway between rings are plotted in Fig. 32. PANDA2 automatically selects the "best" design (with "best" defined as in the discussion associated with Fig. 23).

After optimization via SUPEROPT the values of the decision variables are:

T(1) = 0.42909 in., B(RNG) = 10.87 in., H(RNG) = 7.0240 in., W(RNG) = 4.7606 in., T(2) = 0.20275 in., T(3) = 0.12678 in.

The weight of 180 degrees of the stiffened cylindrical shell is 9892 lbs.

The margins corresponding to the optimum design are listed in Table 5. Notice that in this case all three of the types of skin-ring module buckling are critical at the optimum design. This is unusual and good for the purpose of demonstration. Note that the three margins for buckling of the discretized skin-ring module,

7.59E-03 Inter-ring buckling, discrete model, n=20 circ.halfwaves;FS=0.999

-5.15E-02 Hi-n Ring web buckl.,discrete model, n=53 circ.halfwaves;FS=0.999

8.61E-02 Lo-n Ring sidesway, discrete model, n=3 circ.halfwaves;FS=0.999

are identical for both SUBCASE 1 (midway between rings) and SUBCASE 2 (at rings). For a perfect shell this is as it should be, since the discretized skin-ring module model accounts for the variation in hoop prebuckling resultant, N_y, in the cylindrical skin along the axis of the cylindrical shell.

Different skin-ring module margins would be obtained for SUBCASE 1 and SUBCASE 2 if a general buckling modal initial imperfection were present. The effect of an initial general buckling modal imperfection is accounted for in this new branch of PANDA2 (as it is in the other new branches described in this paper). Corresponding to conditions midway between rings (SUBCASE 1) PANDA2 uses as the general buckling modal imperfection both the sign and the magnitude of the imperfection amplitude supplied by the user in MAINSETUP (*.OPT file). Corresponding to conditions at the rings (SUBCASE 2) PANDA2 reverses the user-supplied sign of the general buckling modal imperfection. In this way, in a single load set, PANDA2 covers both negative and positive initial general buckling modal imperfections.

Table 6 lists margins for this same design, processed before introduction of the discretized skin-ring module into PANDA2.

Table 7 lists the new margins from the discretized skin-ring module model, reproduced from Table 5, and those margins from the old PANDA-type analysis, reproduced from Table 6, that are now superseded for this particular case by the new margins. The old margins are superseded via logic of the type presented in Table 4 for the special case of local buckling of the panel skin.

New PANDA2 Processor, PANEL2, for Evaluation of PANDA2 design via BOSOR4

There now exists a new PANDA2 processor called "PANEL2", analogous to the already existing processor called "PANEL"[1]. "PANEL" sets up a BOSOR4 input file [28] for a multi-module discretized model that includes skin and discretized STRINGER cross sections. The computer program "called" by "PANEL" is BOSPAN (BOSPAN library). The new PANDA2 processor called "PANEL2" sets up a BOSOR4 input file for a multi-module discretized model that includes the panel skin with smeared stringers and discretized RING cross sections. The computer program "called" by "PANEL2" is BOSPN2 (BOSPN2 library).

The new "PANEL2" processor generates a multi-module "skin"-ring input file for BOSOR4 called *.ALL, where "*" indicates the user's name for the case. The "PANEL2" processor requires input from the user analogous to the input required by the skin-stringer processor, "PANEL". This input for "PANEL2" is saved in an annotated file called *.PAN, which is the same name used for the annotated input file for "PANEL". Further details about PANEL2 and the prompting questions and "help" paragraphs that the user of PANEL2 sees are provided in ITEM 463 of [15].

Table 8 lists typical input for the new processor, PANEL2.

Execution of "PANEL2" with the input listed in Table 8 generates a BOSOR4 branched shell model with six skin-ring modules linked together. There are six modules because the user-specified length of the cylindrical shell in Table 8 is 60.54 inches and the optimized ring spacing is 10.09 in., which is one sixth of 60.54.

Figure 33 shows results from the BOSOR4 model thus generated for several different numbers of circumferential waves, n. The predictions of BOSOR4 are in excellent agreement with those from PANDA2 over the entire range of circumferential wavenumber n except for n = 2 (Fig. 33e). The n = 2 prediction from BOSOR4 is low compared to the lowest buckling load predicted from PANDA2 (very close to 1.0) because there is no simple support at the ends of the cylindrical shell in the BOSOR4 model to which Fig. 33e corresponds. Rather, symmetry conditions are applied there. The n = 2 mode shown in Fig. 33e will not be predicted by PANDA2 from the discretized "skin"-ring module model because "global" translation of the single "skin"-ring module is prevented by PANDA2, as mentioned previously. This is done in order to avoid overly conservative predictions for general instability from PANDA2. As mentioned previously, general instability is included via the PANDA-type (smeared ring) model [2] and via the new alternate solution for general instability with discrete stiffeners.

In this case, for which the length of the simply supported cylindrical shell optimized by PANDA2 is 500 inches, it is not possible to set up a BOSOR4 branched shell model 500 inches long because there would be too many individual segments in the BOSOR4 model and also too many degrees of freedom to be within the scope of BOSOR4 [28].

Figure 33a represents the "Ring-sidesway" buckling mode; Figure 33c represents the "Inter-ring" buckling mode; and Figure 33d represents the "Ring web" buckling mode. There is excellent agreement between PANDA2 and BOSOR4 predictions for buckling load factors, cross section mode shapes, and critical circumferential wavenumbers for these three buckling modes.

Figure 33b displays a kind of general instability mode because the lines of intersection of web root and shell skin translate for several of the modules (the four "internal" modules). This short-axial-wave ("high-m") general buckling mode and its associated load factor, 1.095 (equivalent margin = 0.095) predicted by BOSOR4, agree well with the general instability margin and mode shape listed in PART 1 of Table 6:

10 1.25E-01 buck.(SAND);simp-support general buck; M=45;N=4;slope=0.;FS=0.999

CONCLUSIONS

The PANDA2 program for minimum weight design of stiffened panels and shells has been improved by the implementation of three new buckling models:

1. a model based on double trigonometric series expansions of the buckling modal displacement components, u, v, w. This model applies to local buckling of the panel skin between adjacent rings and stringers and to general instability of an unstiffened panel. It is valid for both cylindrical and flat panels under combined in-plane loads, N_x, N_y, N_{xy}, normal pressure p, and thermal loading.

2. a general instability model for ring and stringer stiffened cylindrical panels and shells in which the stiffeners are treated as discrete beam-columns. This model is based on the same type of double trigonometric series expansions for the buckling modal displacement components as used for Item 1.

3. an inter-ring buckling model for ring and stringer stiffened cylindrical panels and shells in which buckling load factors of the skin with smeared stringers and deformable ring segments are obtained from a single discretized "skin"-ring module that is analogous to the discretized skin-stringer module that has long been a part of PANDA2.

These three new buckling models have been tested for configurations that PANDA2 previously had difficulty with, such as laminated angle ply composite plates and shells with few layers in the panel skin and aspect ratios a/b near unity. Now very good agreement is obtained between PANDA2 and STAGS and between PANDA2 and BOSOR4 for unstiffened and stiffened, flat and cylindrical, isotropic and laminated composite panels and cylindrical shells of all the "difficult" types tested so far.

Many of these comparisons are given in the paper. In particular, the new buckling models based on double trigonometric series expansions were tested on several flat and cylindrical unstiffened isotropic and laminated angle-ply panels and on a ring and stringer stiffened angle-ply cylindrical shell subjected to two sets of combined axial compression and in-plane shear loading. The stiffened composite cylindrical shell was optimized with PANDA2 and the optimum design was evaluated with STAGS. The new discretized skin-ring module model was tested through optimization with the new PANDA2 of an internally T-ring stiffened, hydrostatically compressed cylindrical shell and evaluation of the optimum design with BOSOR4.

The BOSOR4 model of the ring-stiffened cylindrical shell optimized by PANDA2 was generated automatically via a new PANDA2 processor called "PANEL2", which is analogous to the PANDA2 processor called "STAGSMODEL" that automatically generates STAGS input files for the analysis of panels optimized by PANDA2 by a general-purpose finite element code.

The results described in the paper qualify PANDA2 for the design of unstiffened and stiffened, flat and cylindrical panels and shells.

ACKNOWLEDGMENTS

David Bushnell very much appreciates the help of his son, Bill Bushnell, in producing the final "double-column" version of the paper required by the AIAA.

REFERENCES

[1] Bushnell, D., "PANDA2 - program for minimum weight design of stiffened, composite, locally buckled panels", Computers and Structures, Vol. 25, pp 469-605, 1987. See also articles: Computer Methods in Appl. Mech. and Engrg, Vol. 103, pp 43-114, 1993; Computers and Structures, Vol. 50, pp 569-602, 1994; Computers and Structures, Vol. 59, pp 489-527, 1996; AIAA Paper 96-1337-CP, AIAA Paper 97-1141; AIAA Paper 97-1142; AIAA Paper 98-1990

[2] Bushnell, D., "Theoretical basis of the PANDA computer program for preliminary design of stiffened panels under combined in-plane loads", Computers and Structures, Vol. 27, pp 541-563, 1987

[3] J. Arbocz and J. Hol, Shell stability analysis in a computer aided engineering (CAE) environment, AIAA Paper 93-133, Proc. 34th AIAA Structures, Structural Dynamics, and Materials Conference, La Jolla, CA, 300-314 (1993).

[4] N. S. Khot and V. B. Venkayya, Effect of fiber orientation on initial postbuckling behavior and imperfection sensitivity of composite cylindrical shells, Air Force Flight Dynamics Laboratory, Wright-Patterson Air Force Base, Ohio, Report AFFDL-TR-70-125, December 1970.

[5] N. R. Bauld, Jr. and N. S. Khot, "A numerical and experimental investigation of the buckling behavior of composite panels", Computers and Structures, 15 (1982) pp. 393-403.

[6] N. S. Khot and N. R. Bauld, Jr., "Further comparison of the numerical and experimental buckling behaviors of composite panels," Computers and Structures, 17, (1983) pp. 61-68.

[7] Timoshenko, S. THEORY OF ELASTIC STABILITY, 1st Edition, McGraw-Hill Book Co., Inc., New York, 1936 (especially pp. 357-361)

[8] Whitney, J. M., STRUCTURAL ANALYSIS OF LAMINATED ANISOTROPIC PLATES, Technomic Publishing Co., Inc., Lancaster, PA, 1987

[9] Jones, R. M., MECHANICS OF COMPOSITE MATERIALS, McGraw-Hill Book CO., New York, 1975

[10] Simitses, G. J. and Ungbhakorn, V., "Minimum-weight design of stiffened cylinders under axial compression", AIAA Journal, Vol. 13, pp 750-755, 1975

[11] Simitses, G. J., "Optimization of stiffened cylindrical shells subjected to destabilizing loads", in STRUCTURAL OPTIMIZATION: STATUS AND PROMISE, Progress in Astronautics and Aeronautics, edited by M. P. Kamat, Vol. 150, AIAA, Washington DC, pp 663-704, 1992

[12] Jaunky, N., Knight, N. F., and Ambur, D. R., "Buckling of arbitrary quadrilateral anisotropic plates",

AIAA Journal, Vol. 33, pp 938-944, 1995

[13] Jaunky, N., Knight, N. F., and Ambur, D. R., "Optimal design of grid-stiffened composite panels using global and local buckling analyses", Journal of Aircraft, Vol. 35, pp 478-486, 1998

[14] Jiang, H., "Analysis and design of composite sandwich panels using PANDA2", Master's degree thesis, Aerospace Engineering Dept., Old Dominion University, Norfolk, VA, August 1998,

[15] Bushnell, D. ITEMs 438, 444, 463 in a computer file, ...panda2/doc/panda2.news, distributed with the PANDA2 computer program, January 1999

[16] Donnell, L. H., "A new theory for the buckling of thin cylinders under axial compression", Trans. Am. Soc. Mech. Eng., Vol. 56, pp 795-806, 1934

[17] Sanders, J. L. Jr., "Nonlinear theories for thin shells", Quarterly Applied Math, Vol. 21, pp 21-36, 1963. Also see, "An improved first-approximation theory for thin shells", NASA TR R-24, Langley Research Center, 1959

[18] Marlowe, M. B. and Flugge, W., "Some new developments in the foundations of shell theory, Lockheed Missiles and Space Company Report LMSC-6-78-68-13, May, 1968

[19] Nemeth, M. P., "Nondimensional parameters and equations for buckling of anisotropic shallow shells", J. Appl. Mech, Vol. 61, pp 664-669, 1994.

[20] Bushnell, D. and Bushnell, W. D., "Approximate method for the optimum design of ring and stringer stiffened cylindrical panels and shells with local, inter-ring and general buckling modal imperfections", Computers and Structures, Vol. 59, pp. 489-527 (1996)

[21] Bushnell, D., "Optimization of composite, stiffened, imperfect panels under combined loads for service in the postbuckling regime", Computer Methods in Applied Mechanics and Engineering, Vol. 103, pp 43-114 (1993)

[22] Almroth, B. O. and Brogan, F. A., "The STAGS computer code", NASA CR-2950, NASA Langley Research Center, Hampton, VA, 1978

[23] Rankin, C. C., Stehlin, P., and Brogan, F. A., "Enhancements to the STAGS computer code", NASA CR-4000, NASA Langley Research center, Hampton, VA, 1986

[24] Bushnell, D. and Bushnell, W. D., "Minimum-weight design of a stiffened panel via PANDA2 and evaluation of the optimized panel via STAGS", Computers and Structures, Vol. 50, pp 569-602, 1994

[25] Bushnell, D., "Recent enhancements to PANDA2", AIAA Paper 96-1337-CP, 37th AIAA Structures, Structural Dynamics and Materials Conference, April, 1996.

[26] Bushnell, D., "Evaluation of various analytical models for buckling and vibration of stiffened shells", AIAA Journal, Vol. 11, No. 9, pp 1283-1291, 1973.

[27] Bushnell, D., COMPUTERIZED BUCKLING ANALYSIS OF SHELLS, Kluwer Academic, Dordrecht, The Netherlands, 1985

[28] Bushnell, D., "BOSOR4: Program for stress, buckling, and vibration of complex shells of revolution," Structural Mechanics Software Series - Vol. 1, (N. Perrone and W. Pilkey, editors), University Press of Virginia, Charlottesville, 1977, pp. 11-131. See also Computers and Structures, Vol. 4, (1974) pp. 399-435; AIAA J, Vol. 9, No. 10, (1971) pp. 2004-2013; Structural Analysis Systems, Vol. 2, A. Niku-Lari, editor, Pergamon Press, Oxford, 1986, pp. 25-54, and Computers and Structures, 18, (3), (1984) pp. 471-536.

Table 1 ADDITIONS TO THE ..panda2/execute/PROMPT.DAT file

```
792.1 Do you want to use the "alternative" buckling solution?
792.2
      The "alternative" buckling solution is more accurate but uses
      much more computer time than the "regular" solution. The "regular"
      solution is the PANDA-type closed form solution obtained from the
      assumed displacement field given by Eqs. (50) in the paper,
      "Theoretical basis...", Computers and Structures, Vol. 27,
      pp 541-563, 1987, leading to Eq. (57) on p. 553 of that paper. The
      "alternative" solution is obtained via double-trig series
      expansions for buckling modal displacement components,  u, v, w.
      It is described in detail in ITEM 438 of ...panda2/doc/panda2.news.

      SUGGESTION: Start optimization by answering "N". Then finalize
      with use of the answer "Y".
```

Table 2 Intermediate results listed in the *.OPM file during computations of buckling of an unstiffened cylindrical composite 4-layered simply supported panel under pure axial compression, Nx = -1.0 lb/in
Dimensions: length=25 in., arc width=6 in., radius=6 in.
Wall construction: [+45,-45,-45,+45]total; ply thickness=0.01 in.
Material: E11=13.75 msi, E22=1.03 msi, G12=G13=G23=0.42 msi, nu(minor)=0.0187273

```
*** BEGIN SUBROUTINE BUCPAN (PANDA-TYPE BUCKLING LOADS) ****
 general buckling: smeared stiffeners
-----------------------------------------------------------------
PART 1: Results from original PANDA-type (closed form) theory [2]:
 ********************** ENTERING GENSTB **********************
 ENTERNG GENSTB: ILABEL,ILABLY,IDESGN,ISAND,INDX,ITHRU,R,A,B=
 7185 9260    0    1    2    1  6.0000E+00  2.5000E+01  6.0000E+00
 Load Set A: Nx,  Ny,  Nxy= -1.0000E+00 -6.0000E-07  5.0000E-03
 Load Set B: Nxo, Nyo, Nxyo=  0.0000E+00  0.0000E+00  0.0000E+00
 EIGMNC=  351.0  351.0  429.0  1.E+17  430.0  351.0  1.E+17
 SLOPEX=  6.39   6.39   0.010  0.00    0.00   6.39   0.00
 MWAVEX=    1      1     24      0      24      1      0
 NWAVEX=    1      1      1      0       1      1      0
 IN GENSTB: MWAVE,NWAVE,CSLOPE,EIGVAL= 1  1  6.0213  3.4775E+02
 Buckling load factor before t.s.d.=347.75; After t.s.d.=339.32
-----------------------------------------------------------------
```

```
PART 2: Results from alternate (double-trig. series) theory:
 Entering ALTSOL: axial, circ. dimensions =  25.000  6.00
 See ITEMs 438, 444  in the file ..panda2/doc/panda2.news .
 *** GENERAL BUCKLING ***
    Number of discrete stringers, rings: NUMSTR, NUMRNG=  0  0

 Entering ALTSOL. MNTOT=  65 = rank of the matrices
 MAMAX,NAMAX,MBMAX,NBMAX,MCMAX,NCMAX,MDMAX,NDMAX,MEMAX,NEMAX=
 5   5   5   5   5   5   5   5   5   5 <--upper limit on trig.
 **** NOTE: The shell is PERFECT ****

 Shell theory indicator, ISANDQ= 1 (Sanders theory)
 critical wave no. and eigenvalue from PANDA-type analysis
                        (with t.s.d.)=  3.3932E+02(CURVED)
 High-m wavenumber and eigenvalue from PANDA-type analysis
                     (without t.s.d.)=  4.2886E+02(CURVED)

 Axial lengths:  (XMAX(i),i=1,KOUNT)=
  2.5000E+01  1.2500E+01  6.2500E+00  3.1250E+00  1.5625E+00
 Load factors: (EIGTRY(i),i=1,KOUNT)=
  4.2340E+02  5.2410E+02  4.4952E+02  3.9736E+02  4.7465E+02

 Entering ALTSOL. MNTOT= 125 <-- rank of matrices
 MAMAX,NAMAX,MBMAX,NBMAX,MCMAX,NCMAX,MDMAX,NDMAX,MEMAX,NEMAX=
 7   7   7   7   7   7   7   7   7   7 <--upper limit on trig.

 EIGODD;EIGEVN=4.1612E+02; 3.9588E+02 <--(m+n) odd; (m+n) even

 Axial length:  (XMAX(i),i=1,KOUNT) = 3.125 in.
 Load factor :  (EIGTRY(i),i=1,KOUNT)= 3.9588E+02

 Critical buckling load before t.s.d.=  3.9588E+02(PERFECT)
 Critical buckling load after  t.s.d.=  3.8499E+02(PERFECT)
 Critical buckling load factor from ALTSOL after  t.s.d.
 and after reduction by a factor of  9.5000E-01 to compensate for
 truncation of double trig. series expansion (perfect shell)=
                                        3.6574E+02(CURVED)(PERFECT)
 Critical buckling load factor
 from orig. PANDA theory (perfect shell)=
                                        3.3932E+02(CURVED)(PERFECT)
 Ratio of ALTSOL eigenvalue to PANDA-type eigenvalue,
                      EIGALT/EIGPAN = 1.078E+00

 General buckling load factor before and after knockdown:
 EIGGNX(before knockdown by 2 factors below)     =3.6574E+02
 Knockdown factor from local modal imperfection =1.0000E+00
 1st modifying factor(no smeared stringers)      =1.0000E+00
 2nd modifyng factor, 1/DENFCT=1 or 1/(EIG9X*FMDKD9)=1.00
 After knockdown, EIGGNX*FKNOCK(9)*FKNMLT/DENFCT=3.6574E+02
 in which
 EIG9X  = lambda(ARBOCZ)/lambda(original PANDA-type theory)
                                                 =1.0034E+00
 where lambda(ARBOCZ)=perfect panel buckling from ARBOCZ theory
 and   lambda(PANDA) =perfect panel buckling from PANDA  theory
 FMDKD9 = 1 or 0.9/EIG9X =  1.0000E+00
 3.65743E+02 buck. load factor simp-support general buck;(0.95*altsol)
 ****  END SUBROUTINE BUCPAN (PANDA-TYPE BUCKLING LOADS) ****
```

Table 3 Margins from PANDA2 for optimized design of ring and stringer stiffened cylindrical shell

Load Set 1:
axial, Nx = -7.00E+02 lb/in; circ., Ny = -1.00E-04 lb/in;
in-plane shear, Nxy = 4.00E+01 lb/in

MARGINS FOR CURRENT DESIGN: LOAD CASE NO. 1, SUBCASE NO. 1 (midbay)

MAR. NO.	MARGIN VALUE	DEFINITION
1	0.309	Inter-ring bucklng, discrete model, n=10 circ.halfwaves;FS
2	1.57	Lo-n Inter-ring buck.,discrete model,n=1 circ.halfwaves;FS
3	51.7	fibertensn:matl=1,SKN,Iseg=2,at:n=6,layer=1,z=-0.0126;-MID
4	58.3	fibercompr:matl=1,SKN,Iseg=2,at:n=6,layer=3,z=0.0063;-MID.
5	48.9	transcompr:matl=1,SKN,Iseg=2,at:n=6,layer=4,z=0.0126;-MID.
6	129.	inplnshear:matl=1,SKN,Iseg=2,at:n=6,layer=2,z=-0.0063;-MID
7	2.69	fibercompr:matl=2,STR,Iseg=3,at:ROOT,layer=1,z=0.;-MID.;FS
8	1.34	buckling margin stringer Iseg.3 . Local halfwaves=10 .MID.
9	0.077	buck.(SAND);simp-support local buck.; (0.95*altsol);FS=1.
10	0.368	buck.(SAND);simp-support smear rings; M=144;N=1;slope=0.05
11	0.125	buck.(SAND);simp-support general buck;M=1;N=2;slope=100.;F
12	6.66E-04	buck.(SAND);simp-support general buck;(0.85*altsol);FS=
13	0.245	buck.(SAND);rolling with local buck.; M=2;N=1;slope=0.09;F
14	0.605	buck.(SAND);rolling with smear rings; M=128;N=1;slope=0.05
15	0.726	buck.(SAND);rolling only of stringers;M=139;N=0;slope=0.;F
16	155.	(Max.allowable ave.axial strain)/(ave.axial strain) -1; FS=

MARGINS FOR CURRENT DESIGN: LOAD CASE NO. 1, SUBCASE NO. 2 (at rings)

MAR. NO.	MARGIN VALUE	DEFINITION
1	0.307	Inter-ring bucklng, discrete model, n=10 circ.halfwaves;F
2	1.57	Lo-n Inter-ring buck.,discrete model,n=1 circ.halfwaves;
3	108.	fibertensn:matl=1,SKN,Iseg=2,at:n=1,layer=4,z=0.0126;-RNGS
4	62.8	fibercompr:matl=1,SKN,Iseg=2,at:n=1,layer=2,z=-0.0063;-RNG
5	49.1	transcompr:matl=1,SKN,Iseg=2,at:n=1,layer=1,z=-0.0126;-RNG
6	132.	inplnshear:matl=1,SKN,Iseg=2,at:n=1,layer=2,z=-0.0063;-RNG
7	31.1	fibertensn:matl=2,RNG,Iseg=3,at:TIP,layer=1,z=0.;-RNGS;FS=
8	2.31	fibercompr:matl=2,STR,Iseg=3,at:TIP,layer=1,z=0.;-RNGS;FS=
9	3.34E-06	buckling margin stringer Iseg.3. Local halfwaves=1 .RN
10	3.28E-03	buck.(SAND);simp-support local buck.; (0.95*altsol);FS=
11	0.354	buck.(SAND);simp-support smear rings; M=144;N=1;slope=0.05
12	9.89E-03	buck.(SAND);rolling with local buck.;M=1;N=1;slope=0.31
13	0.582	buck.(SAND);rolling with smear rings; M=128;N=1;slope=0.05
14	0.5.4	buck.(SAND);rolling only of stringers;M=139;N=0;slope=0.;F
15	156.	(Max.allowable ave.axial strain)/(ave.axial strain) -1; FS

Table 3 (continued)

Load Set 2:
axial, Nx = -1.00E+02 lb/in; circ., Ny = -1.00E-04 lb/in;
in-plane shear, Nxy = 1.50E+02 lb/in

MARGINS FOR CURRENT DESIGN: LOAD CASE NO. 2, SUBCASE NO. 1 (midbay)

MAR. NO.	MARGIN VALUE	DEFINITION
1	1.02	Inter-ring bucklng, discrete model, n=10 circ.halfwaves;FS=0.999
2	0.899	Lo-n Inter-ring buck.,discrete model,n=8 circ.halfwaves;FS=0.999
3	20.7	fibertensn:matl=1,SKN,Iseg=2,at:n=6,layer=1,z=-0.0126;-MID.;FS=1.
4	20.6	fibercompr:matl=1,SKN,Iseg=2,at:n=6,layer=3,z=0.0063;-MID.;FS=1.
5	6000.	transtensn:matl=1,SKN,Iseg=2,at:n=6,layer=2,z=-0.0063;-MID.;FS=1.
6	177.	transcompr:matl=1,SKN,Iseg=2,at:n=6,layer=4,z=0.0126;-MID.;FS=1.
7	214.	inplnshear:matl=1,SKN,Iseg=2,at:n=6,layer=2,z=-0.0063;-MID.;FS=1.
8	24.8	fibercompr:matl=2,STR,Iseg=3,at:ROOT,layer=1,z=0.;-MID.;FS=1.
9	12.3	buckling margin stringer Iseg.3 . Local halfwaves=7 .MID.;FS=1.
10	4.00E-04	buck.(SAND);simp-support local buck.; (0.95*altsol);FS=1.
11	2.40	buck.(SAND);simp-support smear rings; M=144;N=1;slope=0.2469;FS=1.
12	2.25E-04	buck.(SAND);simp-supp. general buck;M=1;N=3;slope=7.7;FS=0.999
13	0.230	buck.(SAND);simp-support general buck;(0.85*altsol);FS=0.999
14	0.066	buck.(SAND);rolling with local buck.; M=5;N=1;slope=0.9856;FS=1.
15	2.86	buck.(SAND);rolling with smear rings; M=134;N=1;slope=0.2848;FS=1.
16	11.1	buck.(SAND);rolling only of stringers;M=139;N=0;slope=0.;FS=1.6
17	1.09E+03	(Max.allowable ave.axial strain)/(ave.axial strain) -1; FS=1.

MARGINS FOR CURRENT DESIGN: LOAD CASE NO. 2, SUBCASE NO. 2 (at rings)

MAR. NO.	MARGIN VALUE	DEFINITION
1	1.17	Inter-ring bucklng, discrete model, n=10 circ.halfwaves;FS=0.999
2	1.05	Lo-n Inter-ring buck.,discrete model,n=8 circ.halfwaves;FS=0.999
3	21.1	fibertensn:matl=1,SKN,Iseg=2,at:n=1,layer=4,z=0.0126;-RNGS;FS=1.
4	20.7	fibercompr:matl=1,SKN,Iseg=2,at:n=1,layer=2,z=-0.0063;-RNGS;FS=1.
5	5730.	transtensn:matl=1,SKN,Iseg=2,at:n=1,layer=3,z=0.0063;-RNGS;FS=1.
6	177.	transcompr:matl=1,SKN,Iseg=2,at:n=1,layer=1,z=-0.0126;-RNGS;FS=1.
7	214.	inplnshear:matl=1,SKN,Iseg=2,at:n=1,layer=2,z=-0.0063;-RNGS;FS=1.
8	217.	fibertensn:matl=2,RNG,Iseg=3,at:TIP,layer=1,z=0.;-RNGS;FS=1.
9	22.5	fibercompr:matl=2,STR,Iseg=3,at:TIP,layer=1,z=0.;-RNGS;FS=1.
10	11.3	buckling margin stringer Iseg.3 . Local halfwaves=7 .RNGS;FS=1.
11	-0.0124	buck.(SAND);simp-support local buck.; (0.95*altsol);FS=1.
12	2.40	buck.(SAND);simp-support smear rings; M=144;N=1;slope=0.2469;FS=1.
13	5.02E-02	buck.(SAND);rolling with local buck.; M=5;N=1;slope=0.9856;FS=1.
14	2.85	buck.(SAND);rolling with smear rings; M=134;N=1;slope=0.2792;FS=1.
15	10.3	buck.(SAND);rolling only of stringers;M=139;N=0;slope=0.;FS=1.6
16	1100.	(Max.allowable ave.axial strain)/(ave.axial strain) -1; FS=1.

Table 4 Edited fragment of the *.OPM file listed by PANDA2 for a hydrostatically compressed, ring-stiffened cylindrical shell. Buckling is from the PANDA-type (closed form) solution.

```
*** BEGIN SUBROUTINE BUCPAN (PANDA-TYPE BUCKLING LOADS) ****
 Local buckling, C11=  4.7154E+06, radius, R=  1.0000E+02
 ENTERNG GENSTB: ILABEL,ILABLY,IDESGN,ISAND,INDX,ITHRU,R,A,B=
 7010 9260    0    0    1    1  1.0000E+02  1.0090E+01  3.1400E+02
 Load Set A: Nx,  Ny,  Nxy= -1.0000E+04 -1.5361E+04  1.1180E+02
 Load Set B: Nxo, Nyo, Nxyo=  0.0000E+00  0.0000E+00  0.0000E+00
 EIGMNC=  0.989  0.989  0.989  1.E+17  1.E+17  1.05  1.E+17
 SLOPEX=  0.00   0.00   0.00   0.00    0.00    0.00  0.00
 MWAVEX=     1      1      1      0       0       1     0
 NWAVEX=    18     18     18      0       0      10     0
 IN GENSTB: MWAVE,NWAVE,CSLOPE,EIGVAL=  1, 18  0.0000  0.98934

 Simple-support local buckling between adjacent rings
 is not recorded as a margin because this type of buckling
 has been superceded by the results from the discretized
 skin-ring module model, for which skin-ring buckling
 load factors have been computed in the range from n =   1
 to n =  76 circumferential halfwaves.
 The critical simple-support inter-ring buckling model has 18
 circ. half waves, which lies within this range.
```

Table 5 Margins for optimized hydrostatically compressed isotropic internally T-ring stiffened cylindrical shell generated with the new discretized skin-ring module incorporated into PANDA2

```
PART 1 Margins corresponding to conditions midway between rings:
 MARGINS FOR CURRENT DESIGN: LOAD CASE NO. 1, SUBCASE NO. 1
 MAR. MARGIN
 NO.  VALUE                DEFINITION
  1  0.060 -.05+(eig(high-axial-m) -eig(low-axial-m))/eig(high-m),
  2  0.0076 Inter-ring bucklng, discrete model,n=20 circ.halfwaves,
  3 -0.0515 Hi-n Ring web buckl,discrete model,n=53 circ.halfwaves;.
  4  0.0861 Lo-n Ring sidesway, discrete model, n=3   circ.halfwaves,
  5  4.41   eff.stress:matl=1,SKN,Iseg=1,allnode,layer=1,z=-0.2146;-MID
  6  1.15   buckling   ring   Iseg 4 as beam on foundation. M=250;MID.
  7  1.10E-04 buck.(DONL);simp-support general buck;M=1;N=2;slope=0.;
  8  0.0440 buck.(DONL);   RINGS:    web buckling;M=41;N=1;slope=0.;
  9  795.0  (Max.allowable ave.axial strain)/(ave.axial strain) -1;
 10  0.125  buck.(SAND);simp-support general buck;M=45;N=4;slope=0.;
-----------------------------------------------------------------------

PART 2 Margins corresponding to conditions at the ring locations:
 MARGINS FOR CURRENT DESIGN: LOAD CASE NO. 1, SUBCASE NO. 2
 MAR. MARGIN
 NO.  VALUE                DEFINITION
  1  0.0076 Inter-ring bucklng, discrete model,n=20 circ.halfwaves;FS=0.999
  2 -0.0515 Hi-n Ring web buckl,discrete model,n=53 circ.halfwaves;FS=0.999
  3  0.0861 Lo-n Ring sidesway, discrete model, n=3   circ.halfwaves;FS=0.999
  4  3.53   eff.stress:matl=1,RNG,Iseg=4,allnode,layer=1,z=-0.0634;-RNGS;FS=1.
  5  0.0442 buckling margin   ring   Iseg.3 . Local halfwaves=44 .RNGS;FS=1.
  6  1.15   buckling   ring   Iseg 4 as beam on foundation. M=250;RNGS;FS=3.
  7  0.430  buck.(DONL);rolling only axisym.rings;M=0;N=0;slope=0.;FS=1.6
  8  0.0440 buck.(DONL);   RINGS:    web buckling;M=41;N=1;slope=0.;FS=1.
  9  770.0  (Max.allowable ave.axial strain)/(ave.axial strain) -1; FS=1.
```

Table 6 Margins for the same design to which Table 5 corresponds generated WITHOUT the new discretized skin-ring module incorporated into PANDA2

```
PART 1  Margins corresponding to conditions midway between rings:
 MARGINS FOR CURRENT DESIGN: LOAD CASE NO. 1, SUBCASE NO. 1    (Midbay)
 MAR. MARGIN
 NO.  VALUE                DEFINITION
  1  0.060 -.05+(eig(high-axial-m) -eig(low-axial-m))/eig(high-m);FS=1.
  2  4.41  eff.stress:matl=1,SKN,Iseg=1,allnode,layer=1,z=-0.2146;-MID.;FS=1.
  3  1.15  buckling   ring   Iseg 4 as beam on foundation. M=250;MID.;FS=3.
  4 -0.0107 buck.(DONL);simp-support local buck.; M=1;N=18;slope=0.;FS=1.
  5  0.0001 buck.(DONL);simp-support general buck;M=1;N=2;slope=0.;FS=0.999
  6  0.0615 buck.(DONL);rolling with local buck.; M=1;N=6;slope=0.;FS=1.
  7  0.0440 buck.(DONL);   RINGS:    web buckling;M=41;N=1;slope=0.;FS=1.
  8  795.0  (Max.allowable ave.axial strain)/(ave.axial strain) -1; FS=1.
  9 -0.0109 buck.(SAND);simp-support local buck.; M=1;N=18;slope=0.;FS=1.
 10  0.125  buck.(SAND);simp-support general buck;M=45;N=4;slope=0.;FS=0.999
 11  0.0621 buck.(SAND);rolling with local buck.; M=1;N=6;slope=0.;FS=1.
-----------------------------------------------------------------------

PART 2  Margins corresponding to conditions at ring locations:
 MARGINS FOR CURRENT DESIGN: LOAD CASE NO. 1, SUBCASE NO. 2    (At rings)
 MAR. MARGIN
 NO.  VALUE                DEFINITION
  1  3.53  eff.stress:matl=1,RNG,Iseg=4,allnode,layer=1,z=-0.0634;-RNGS;FS=1.
  2  0.0442 buckling margin   ring   Iseg.3 . Local halfwaves=44 .RNGS;FS=1.
  3 -0.491  buckling margin   ring   Iseg.4 . Local halfwaves=44 .RNGS;FS=1.
  4 -0.309  buckling  ring  Isegs.3+4 together.M=42 ;C=0.     ;RNGS;FS=1.4
  5  1.15   buckling   ring   Iseg 4 as beam on foundation. M=250;RNGS;FS=3.
  6  0.0062 buck.(DONL);simp-support local buck.; M=1;N=18;slope=0.;FS=1.
  7  0.0638 buck.(DONL);rolling with local buck.; M=1;N=6;slope=0.;FS=1.
  8  0.307  buck.(DONL);rolling only of   rings;  M=0;N=3;slope=0.;FS=1.6
  9 -0.102  buck.(DONL);hiwave roll. of   rings;  M=0;N=58;slope=0.;FS=1.2
 10  0.430  buck.(DONL);rolling only axisym.rings;M=0;N=0;slope=0.;FS=1.6
 11  0.044  buck.(DONL);   RINGS:    web buckling;M=41;N=1;slope=0.;FS=1.
 12  770.0 (Max.allowable ave.axial strain)/(ave.axial strain) -1; FS=1.
 13  0.0060 buck.(SAND);simp-support local buck.; M=1;N=18;slope=0.;FS=1.
 14  0.0645 buck.(SAND);rolling with local buck.; M=1;N=6;slope=0.;FS=1.
```

Table 7 New margins from the discretized skin-ring module model and the old PANDA-type margins that have been superceded by them in this particular case of an optimized hydrostatically compressed T-ring-stiffened cylindrical shell

```
PART 1 Margins corresponding to conditions midway between rings:
 SKIN-RING MARGINS FOR CURRENT DESIGN: LOAD CASE NO. 1, SUBCASE NO. 1
 MAR. MARGIN
 NO.  VALUE                DEFINITION
 2   0.0076 Inter-ring bucklng, discrete model,n=20 circ.halfwaves;FS=0.999
 3  -0.0515 Hi-n Ring web buckl,discrete model,n=53 circ.halfwaves;FS=0.999
 4   0.0861 Lo-n Ring sidesway, discrete model,n= 3 circ.halfwaves;FS=0.999
-------------------------------------------------------------------------
PART 2 Margins corresponding to conditions midway between rings:
 OLD PANDA-TYPE MARGINS THAT ARE SUPERCEDED IN THIS CASE BY THE MARGINS
 LISTED IN PART 1
 MAR. MARGIN
 NO.  VALUE                DEFINITION
 4  -0.0107 buck.(DONL);simp-support local buck.; M=1;N=18;slope=0.;FS=1.
 6   0.0615 buck.(DONL);rolling with local buck.; M=1;N=6;slope=0.;FS=1.
 9  -0.0109 buck.(SAND);simp-support local buck.; M=1;N=18;slope=0.;FS=1.
11   0.0621 buck.(SAND);rolling with local buck.; M=1;N=6;slope=0.;FS=1.
-------------------------------------------------------------------------

PART 3 Margins corresponding to conditions at the ring locations:
 SKIN_RING MARGINS FOR CURRENT DESIGN: LOAD CASE NO. 1, SUBCASE NO. 2
 MAR. MARGIN
 NO.  VALUE                DEFINITION
 1   0.0076 Inter-ring bucklng, discrete model,n=20 circ.halfwaves;FS=0.999
 2  -0.0515 Hi-n Ring web buckl,discrete model,n=53 circ.halfwaves;FS=0.999
 3   0.0861 Lo-n Ring sidesway, discrete model, n=3 circ.halfwaves;FS=0.999
-------------------------------------------------------------------------
PART 4 Margins corresponding to conditions at the ring locations:
 OLD PANDA-TYPE MARGINS THAT ARE SUPERCEDED IN THIS CASE BY THE MARGINS
 LISTED IN PART 3
 MAR. MARGIN
 NO.  VALUE                DEFINITION
 3  -0.491  buckling margin ring Iseg.4 . Local halfwaves=44 .RNGS;FS=1.
 4  -0.309  buckling   ring Isegs.3+4 together.M=42 ;C=0.  ;RNGS;FS=1.4
 6   0.0062 buck.(DONL);simp-support local buck.; M=1;N=18;slope=0.;FS=1.
 7   0.0638 buck.(DONL);rolling with local buck.; M=1;N=6;slope=0.;FS=1.
 8   0.307  buck.(DONL);rolling only of   rings;  M=0;N=3;slope=0.;FS=1.6
 9  -0.102  buck.(DONL);hiwave roll. of   rings;  M=0;N=58;slope=0.;FS=1.2
13   0.006  buck.(SAND);simp-support local buck.; M=1;N=18;slope=0.;FS=1.
14   0.0645 buck.(SAND);rolling with local buck.; M=1;N=6;slope=0.;FS=1.
=========================================================================
```

Table 8 *.PAN file, which represents input to the new PANDA2 processor called "PANEL2"

```
-------------------------------------------------------------
  n       $ Do you want a tutorial session and tutorial output?
 60.540   $ Length of the ring-stiffened cylindrical shell, L1
    1     $ Choose BOSOR4 model: INDIC=1 or INDIC=4; INDIC
 -10000.  $ Axial resultant Nx in Load Set A, Nx
    0     $ Axial resultant Nxo in Load Set B, Nxo
  -200    $ Normal pressure p
    1     $ IABP = 1 if pressure in Load Set A; IABP=0 otherwise.
    0     $ Enter control (0 or 1) for rings at the cylinder ends
    1     $ Enter control (1=sym; 2=s.s.; 3=clamp) for buckling b.c.
    2     $ Starting number of circumferential waves [see H(elp)],NOB
   25     $ Ending number of circumferential waves [see H(elp)],NMAXB
    1     $ Increment in number of circumferential waves, INCRB
    1     $ Number of eigenvalues for each circ. wavenumber, NVEC
-------------------------------------------------------------
```

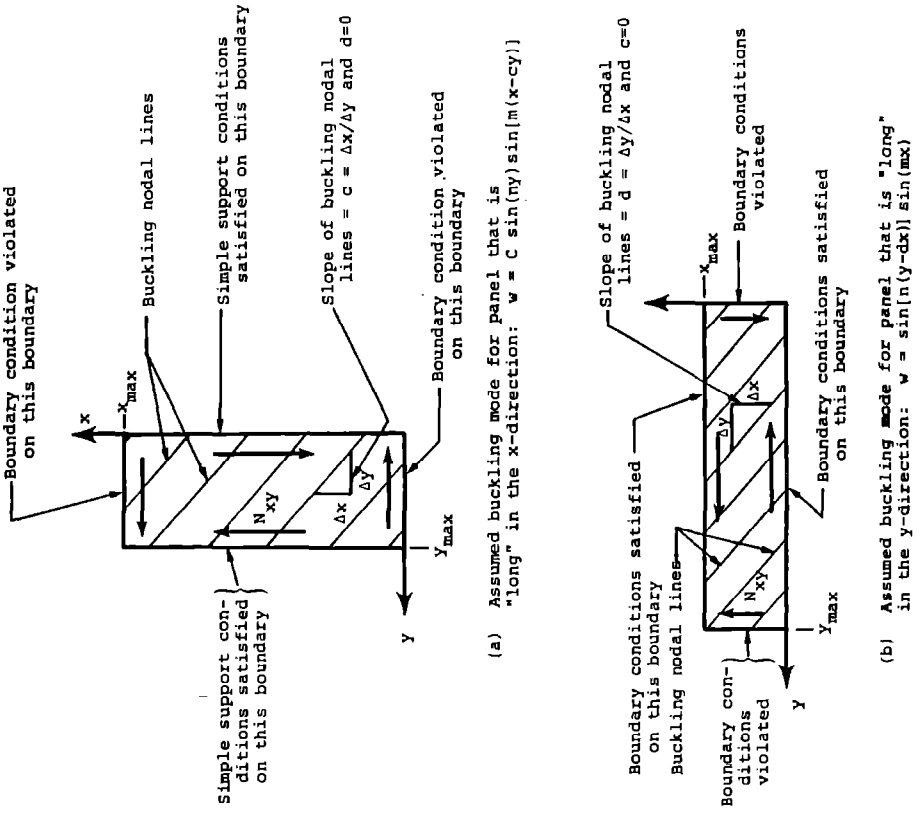

FIG. 2

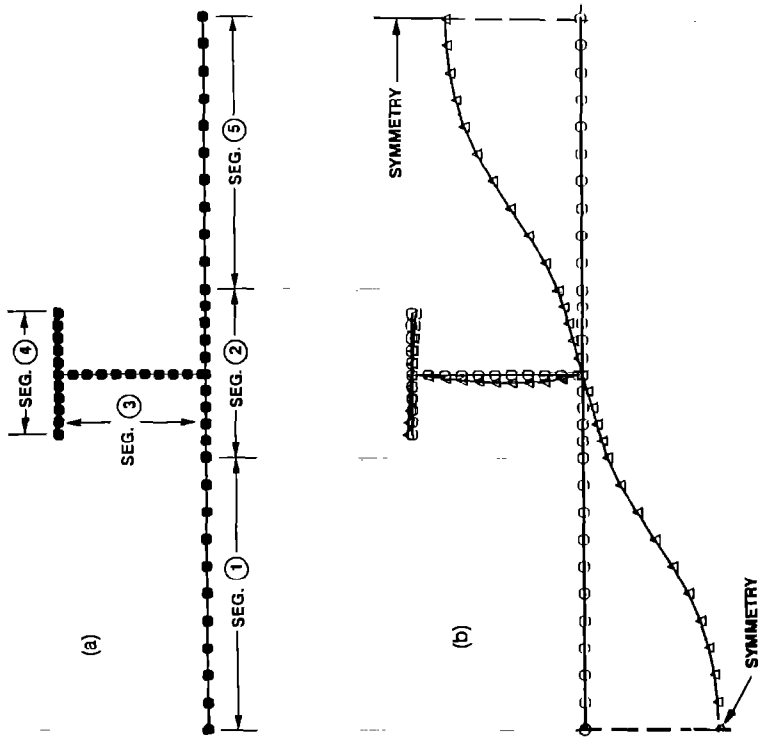

FIG. 1

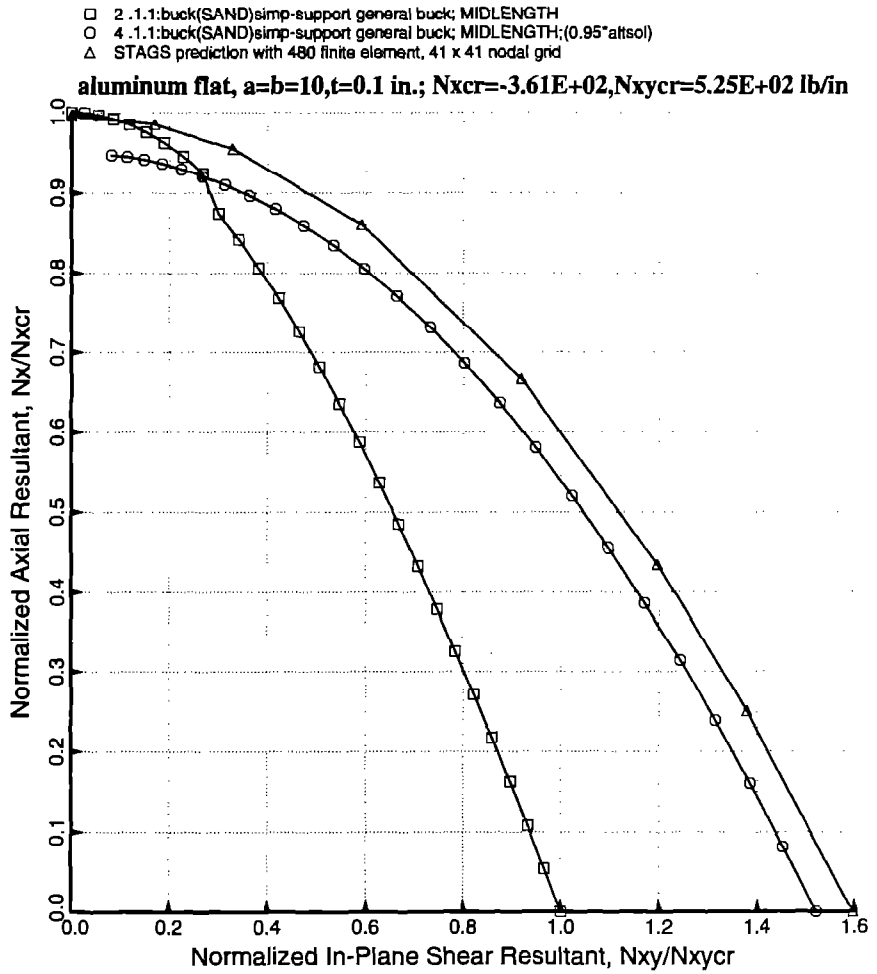

FIG. 3

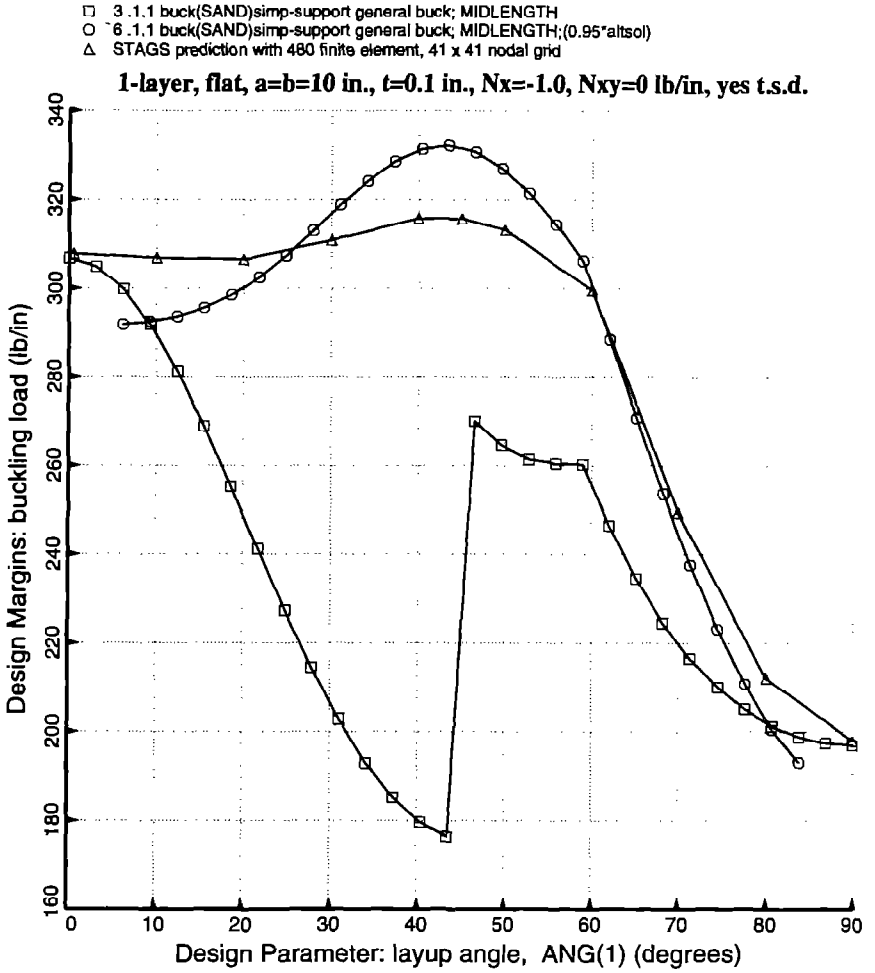

FIG. 4

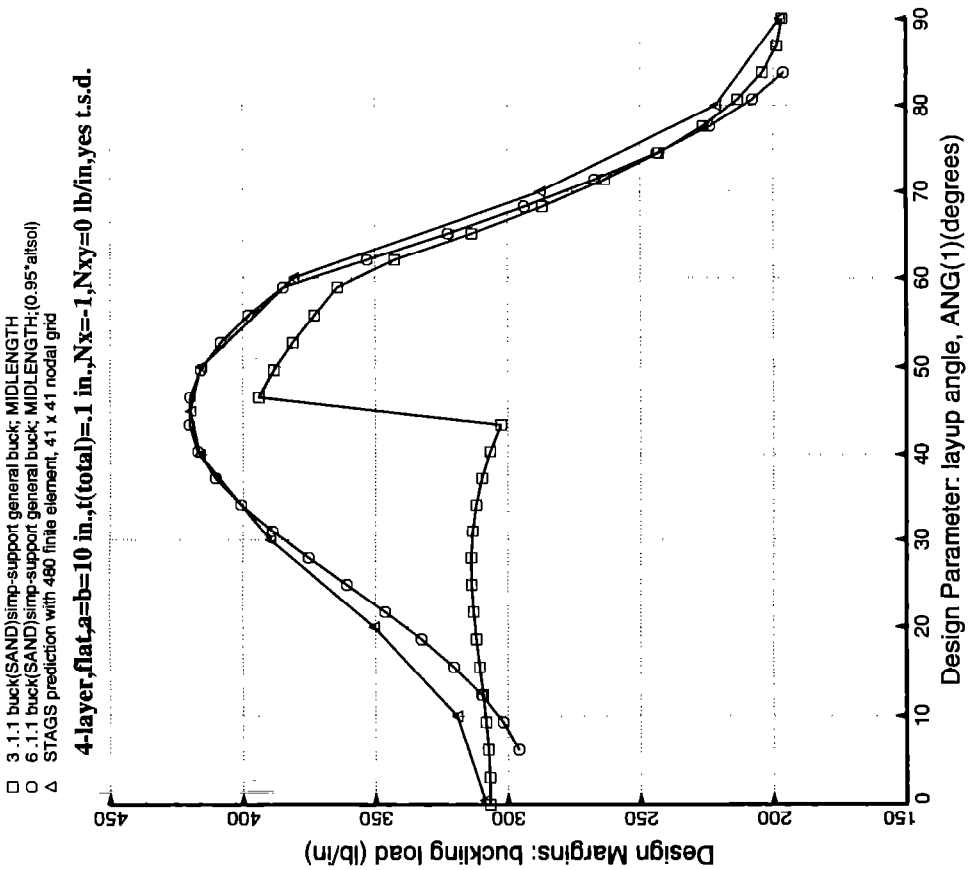

FIG. 6

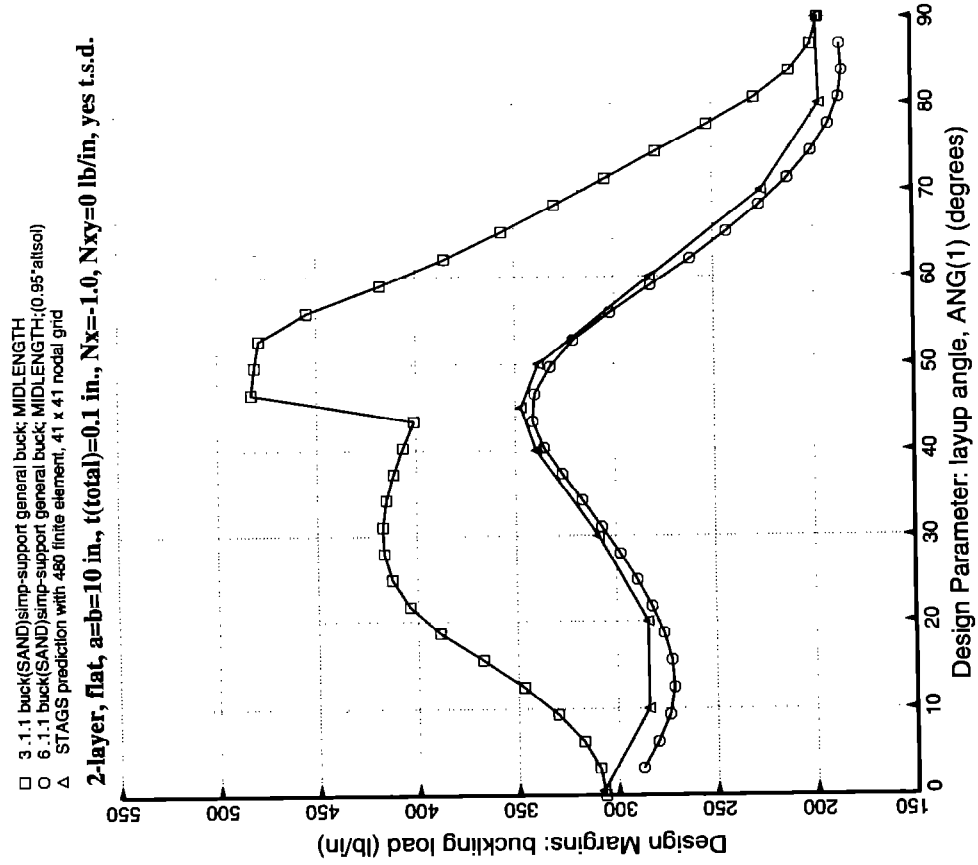

FIG. 5

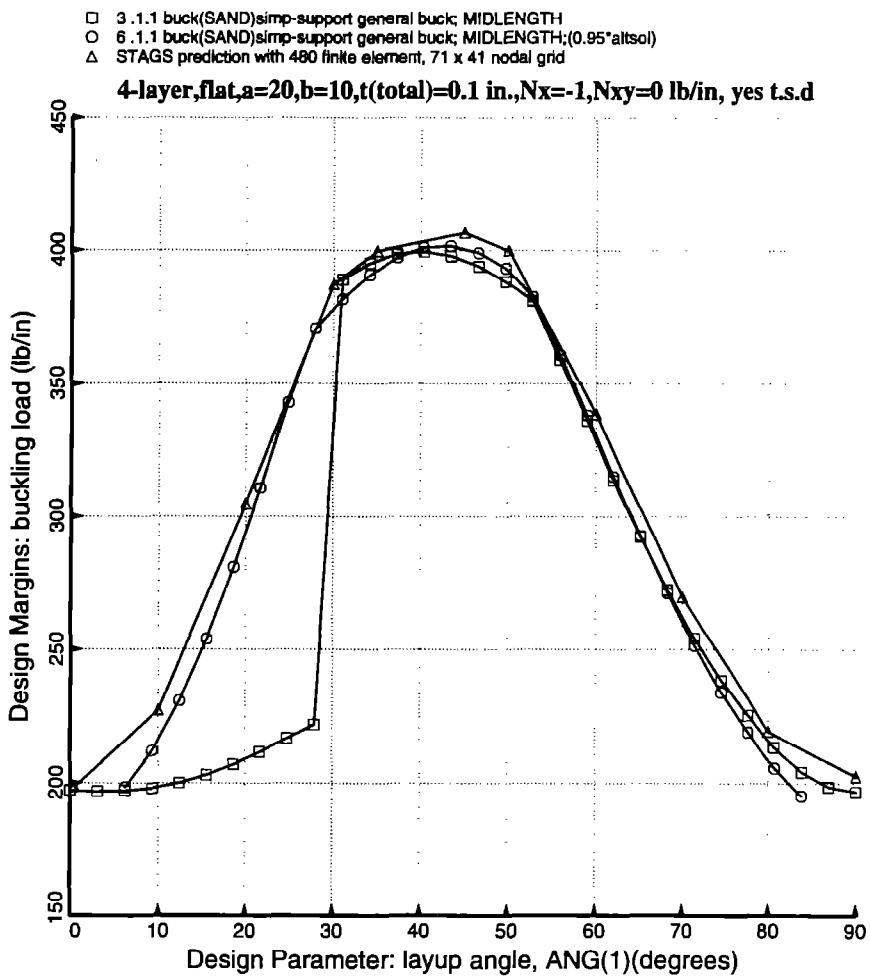

FIG. 7

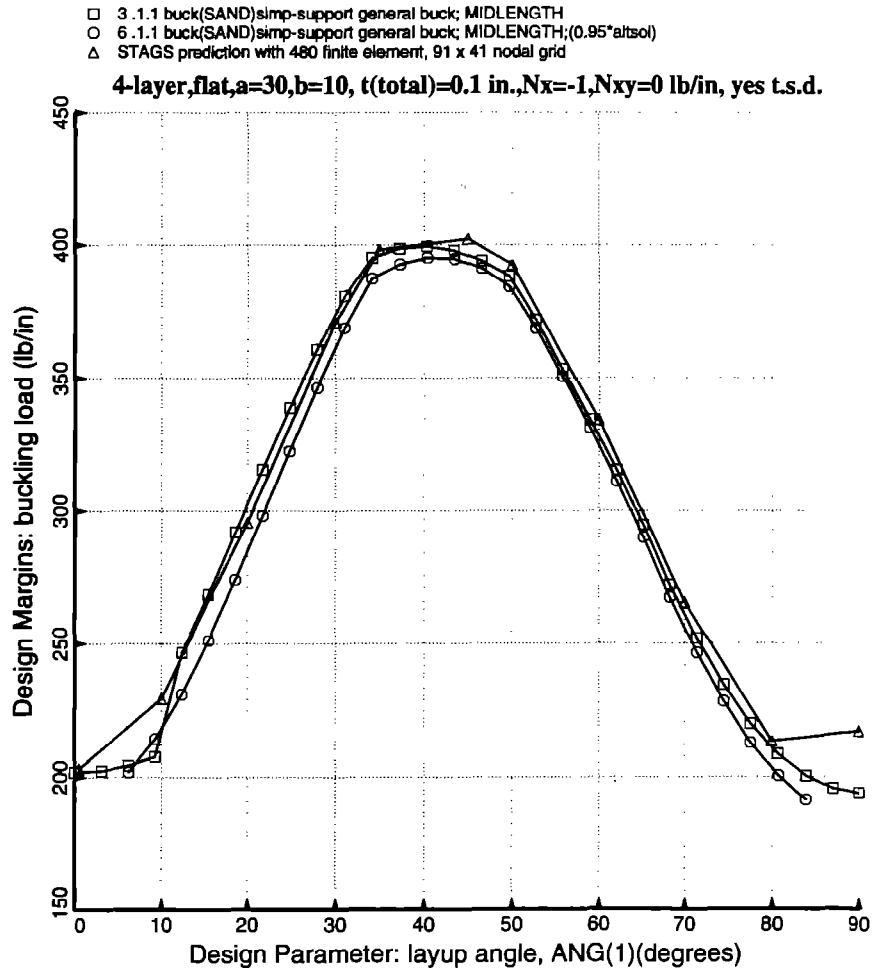

FIG. 8

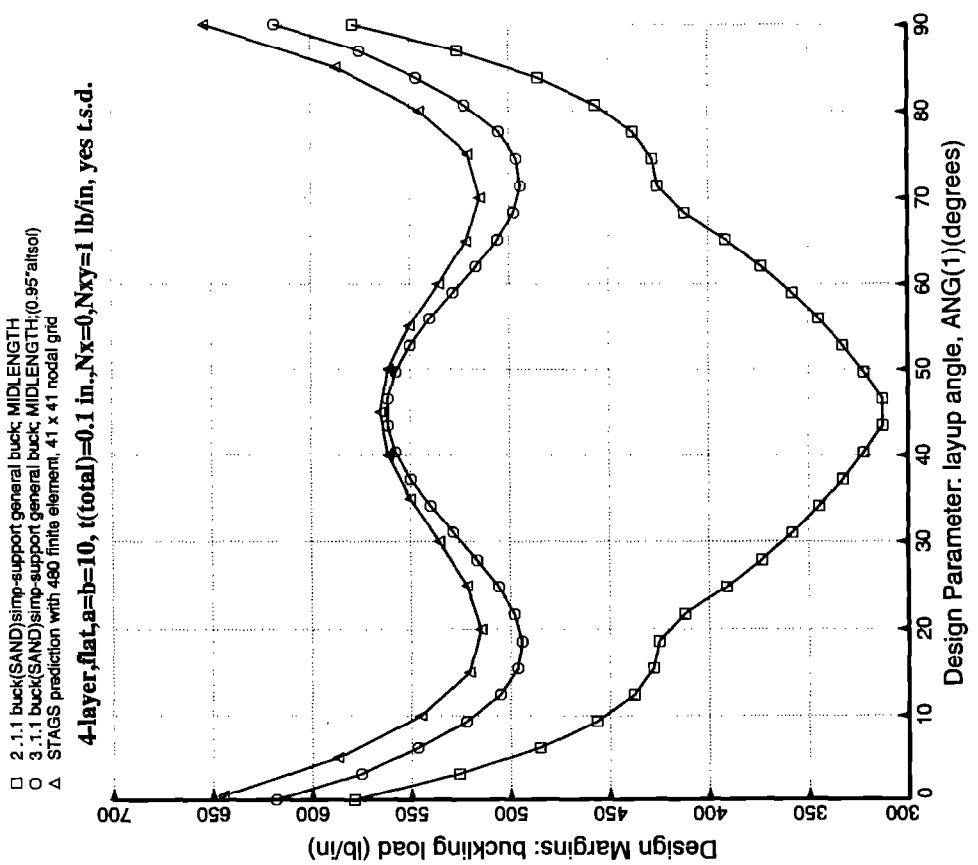

FIG. 9

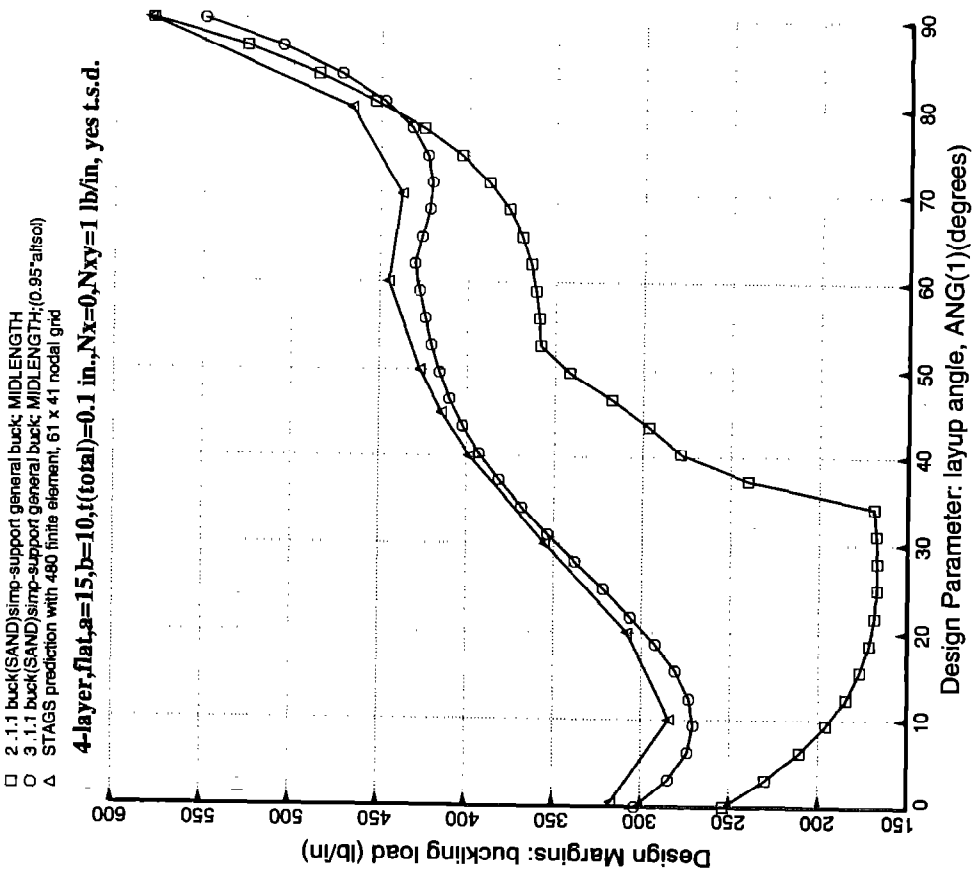

FIG. 10

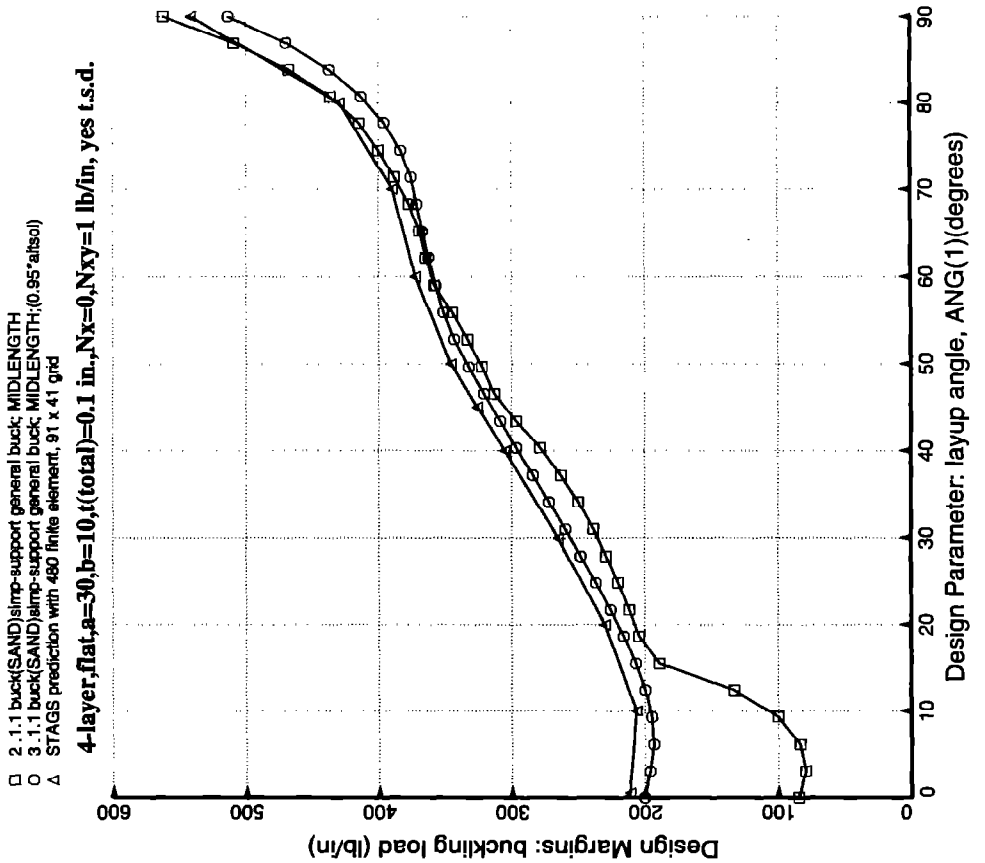

FIG. 12

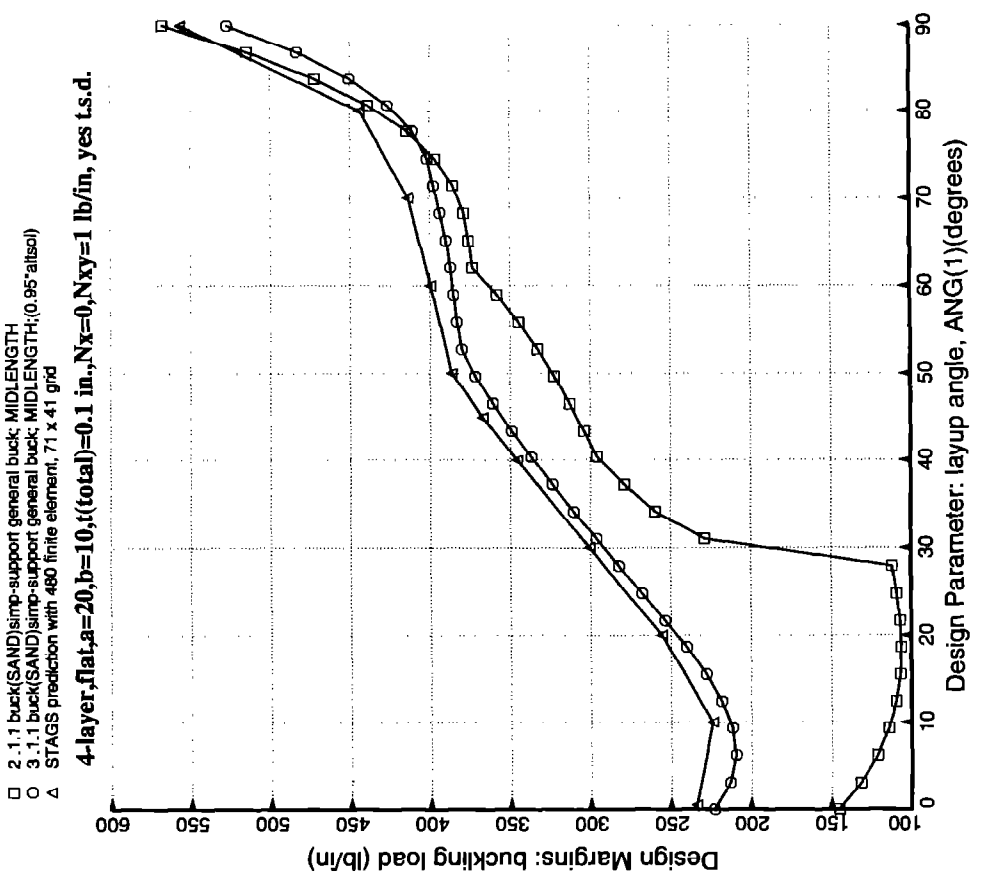

FIG. 11

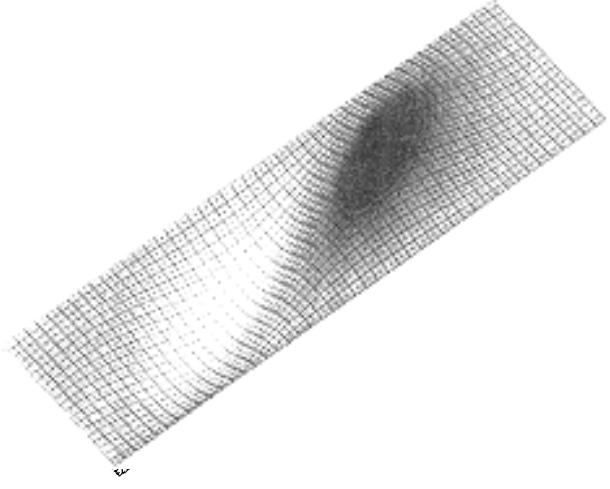

solution scale = 0.2580E+01
mode 1, pcr = 0.32562E+03
step 0 eigenvector w contours
4-layer,flat:a=30,b=10 in., 45 deg., Nx=-0 lb/in, Nxy = 1 lb/in

FIG. 13

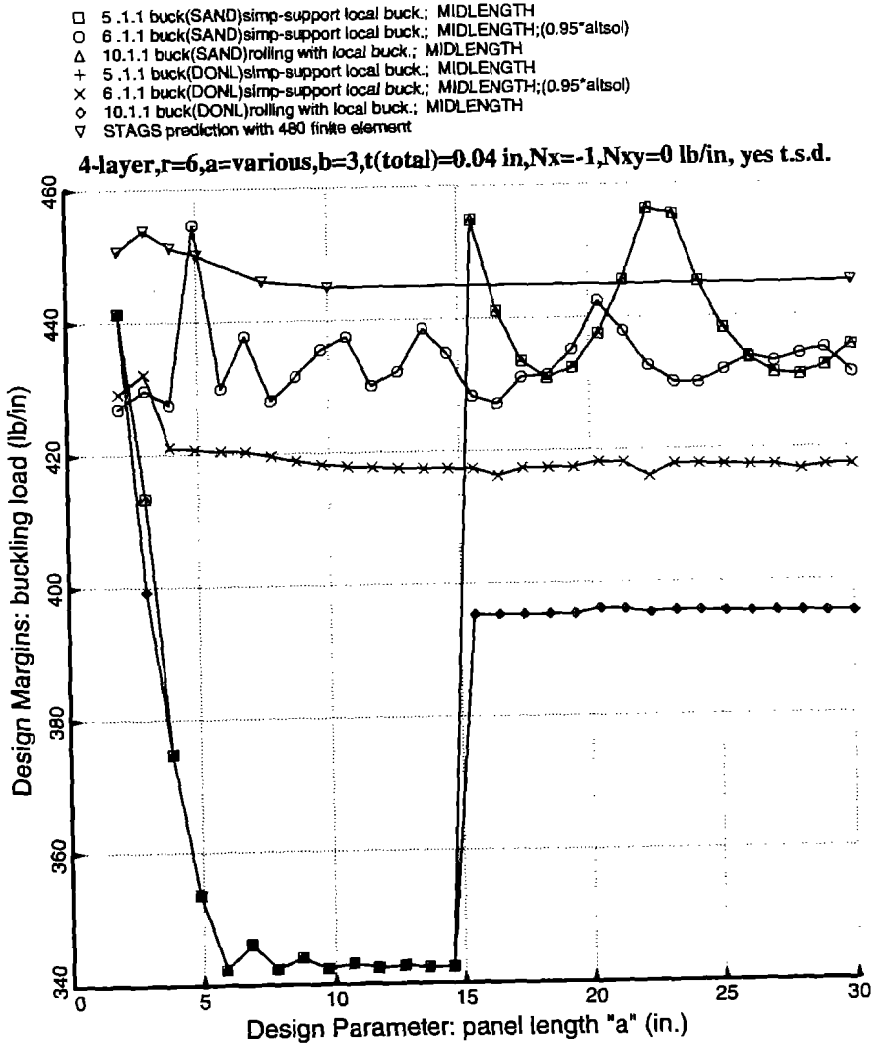

FIG. 14

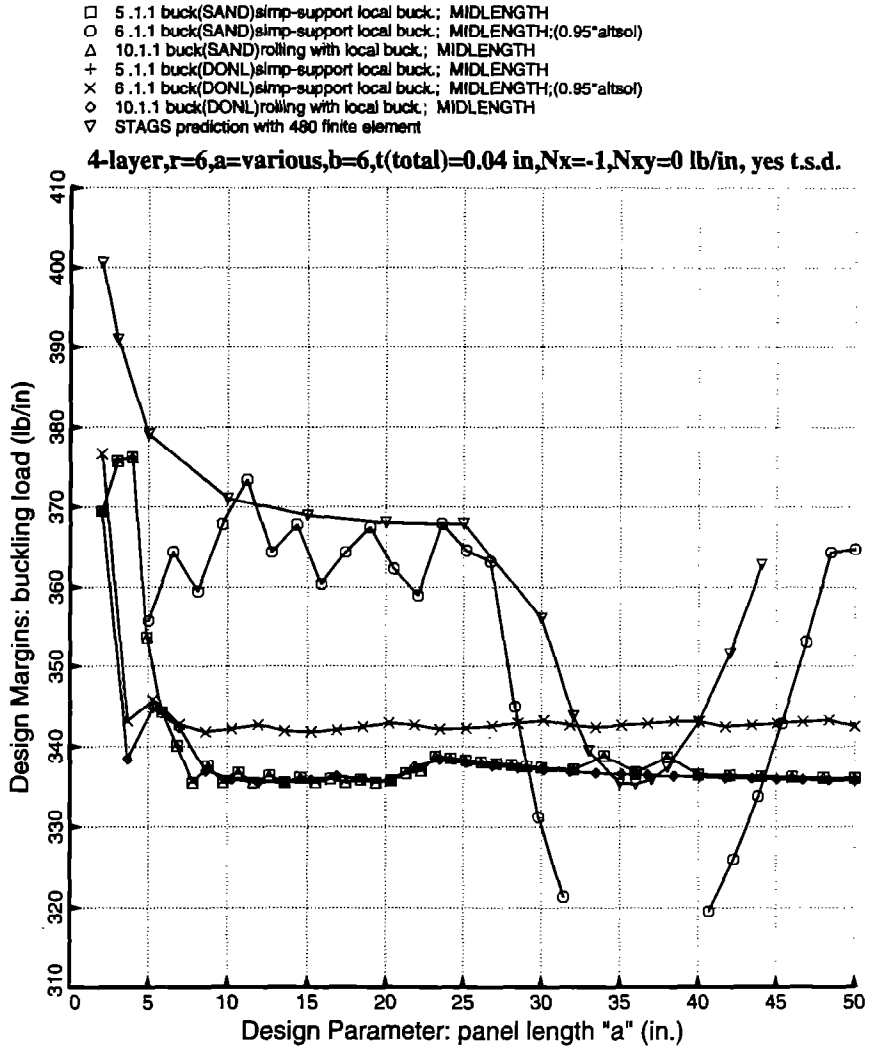

FIG. 15

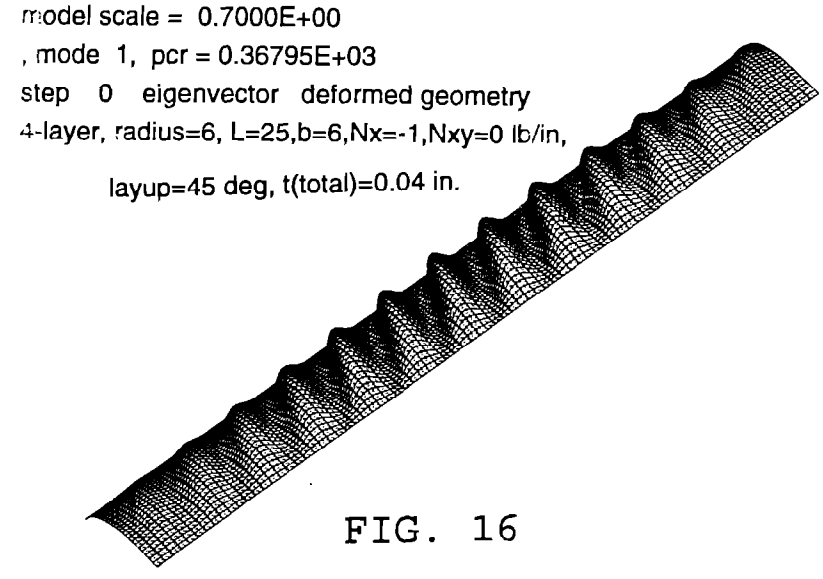

FIG. 16

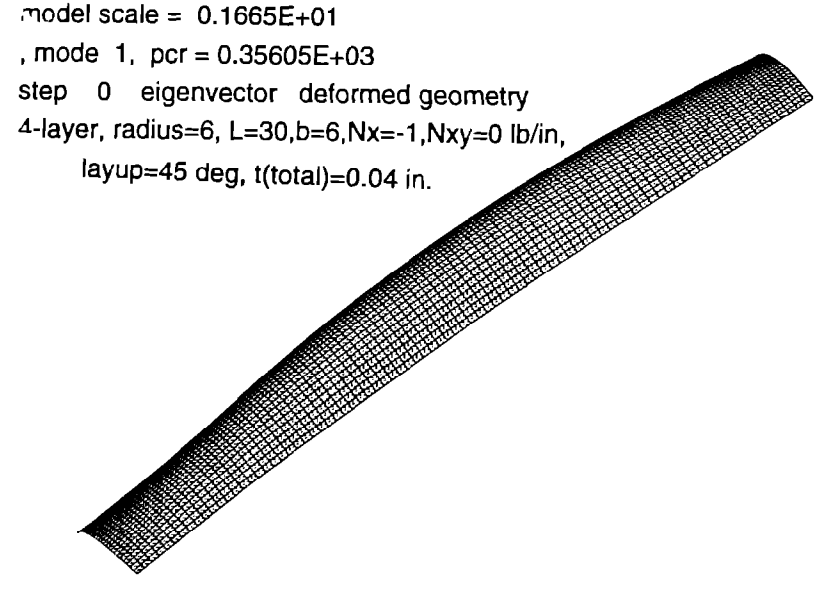

FIG. 17

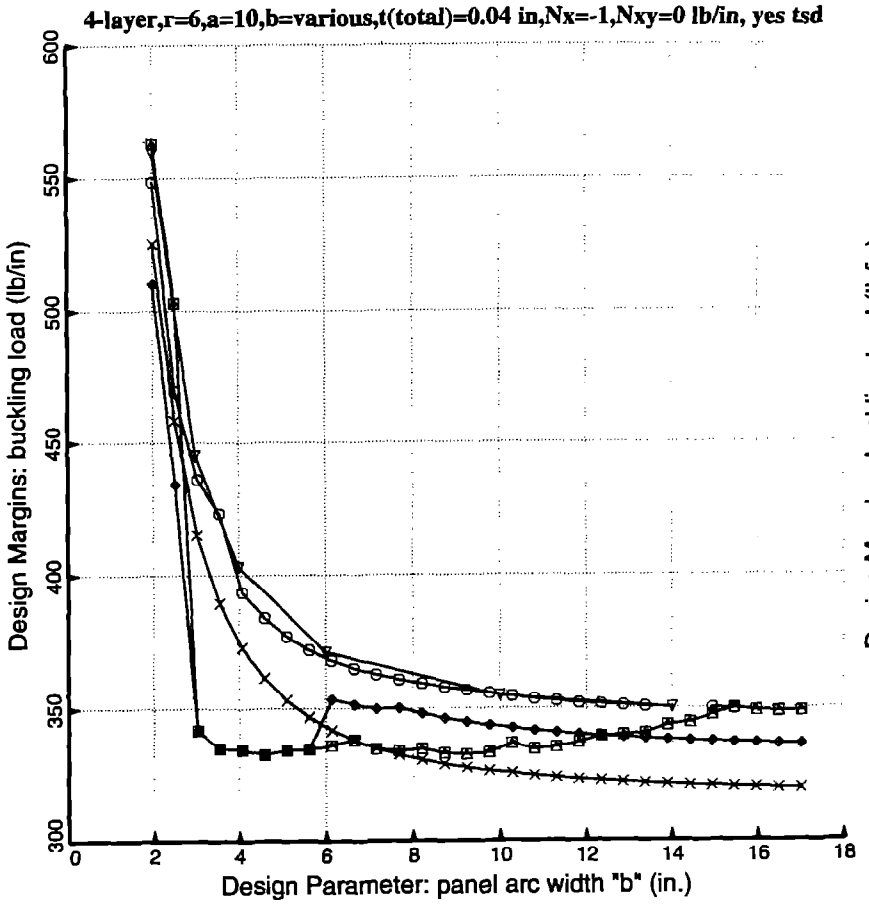

FIG. 18

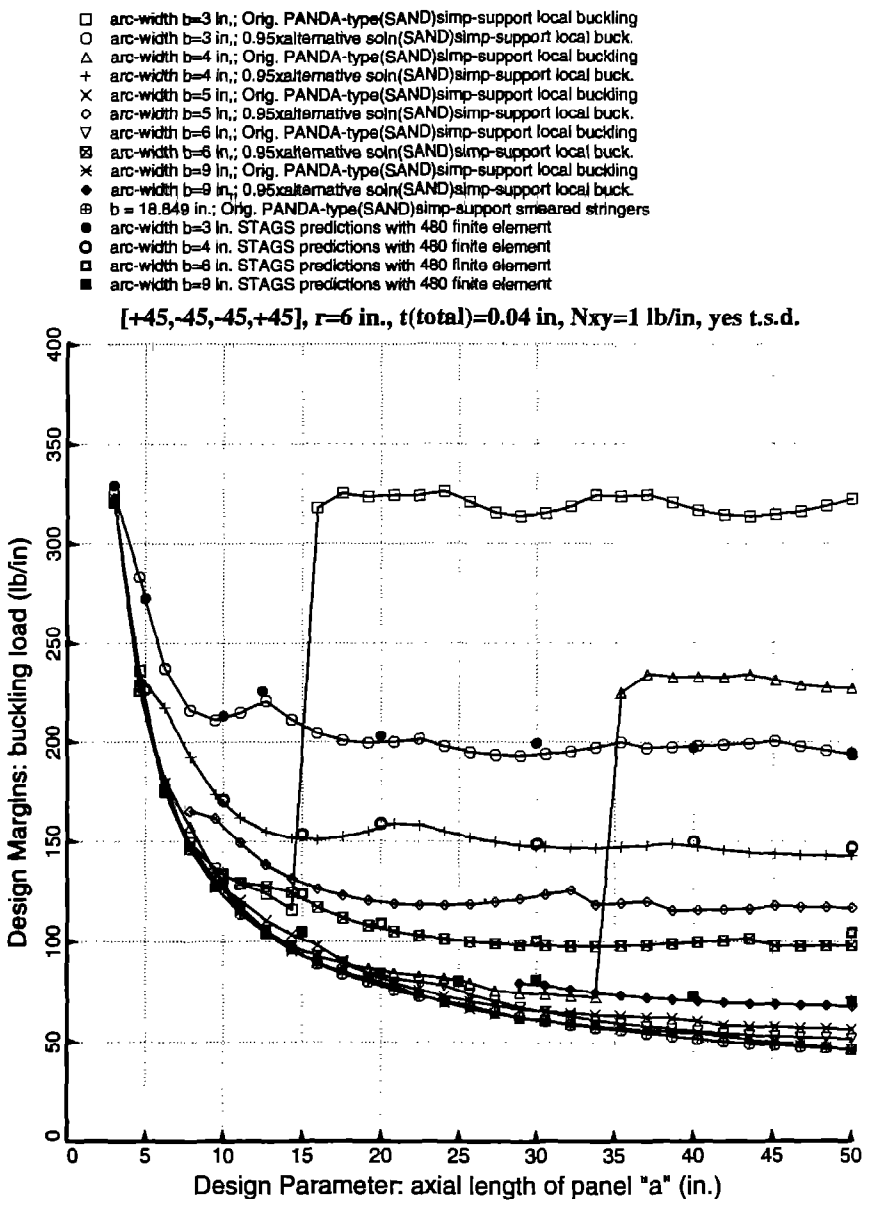

FIG. 19

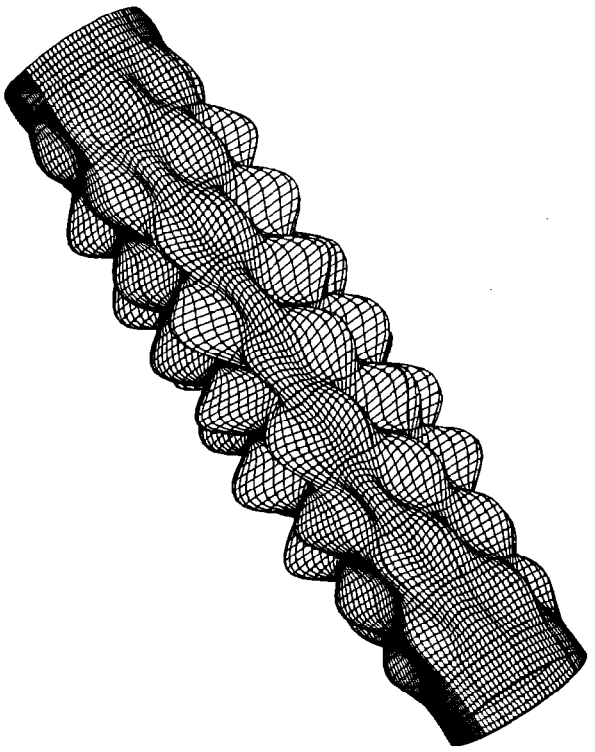

FIG. 21

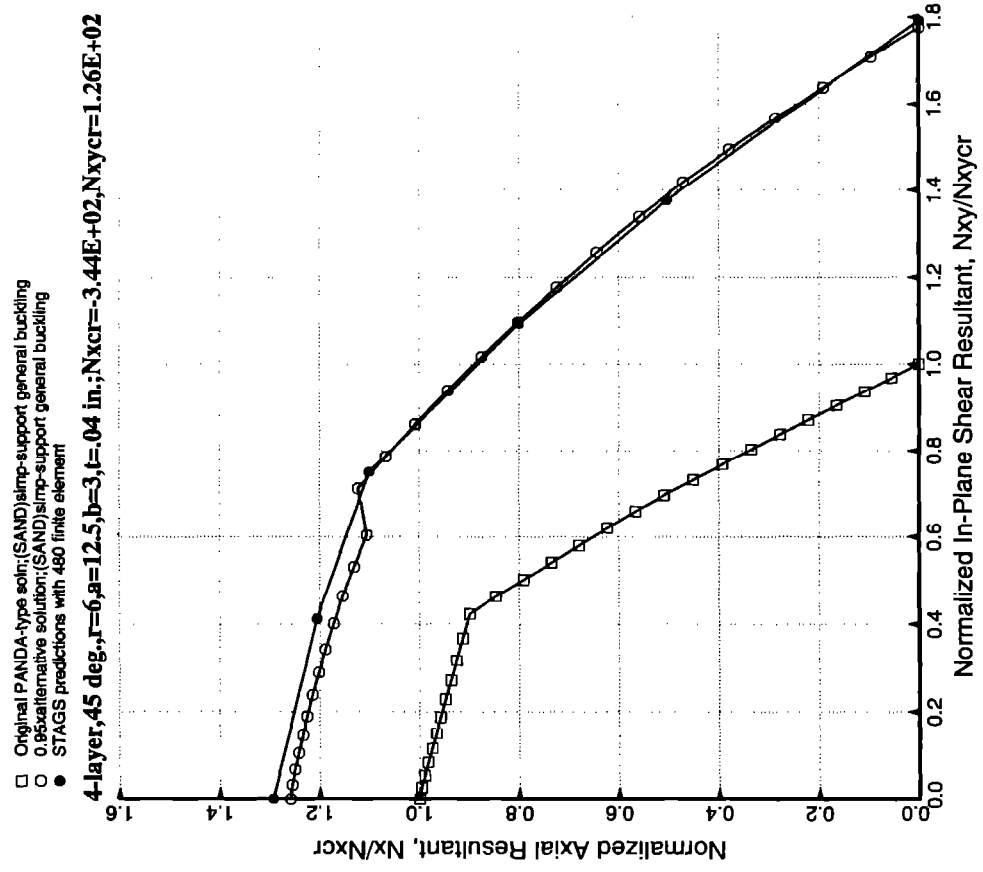

FIG. 20

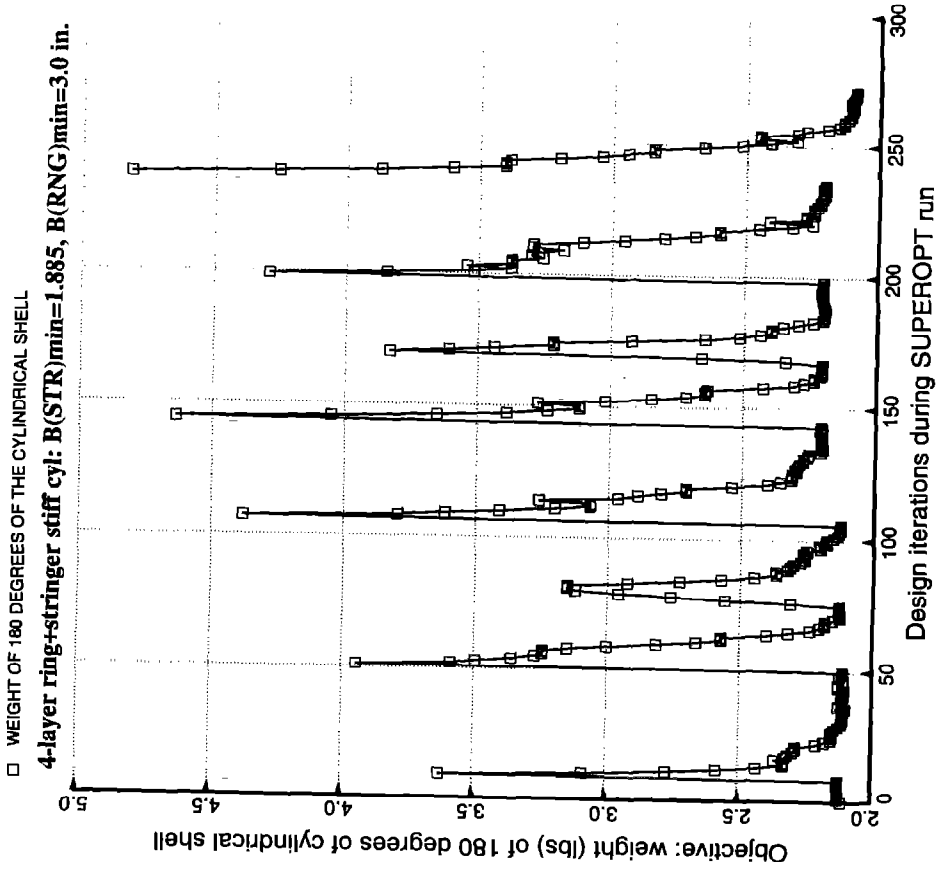

FIG. 23

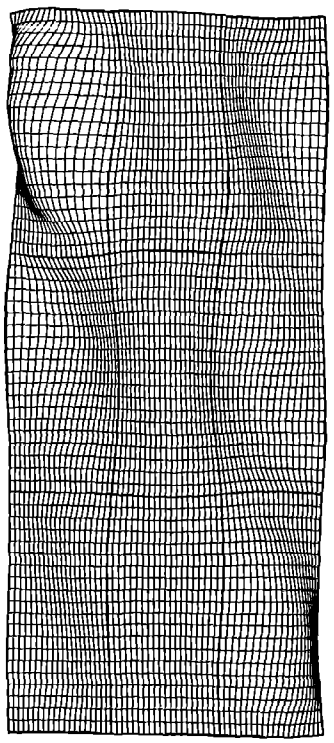

FIG. 22

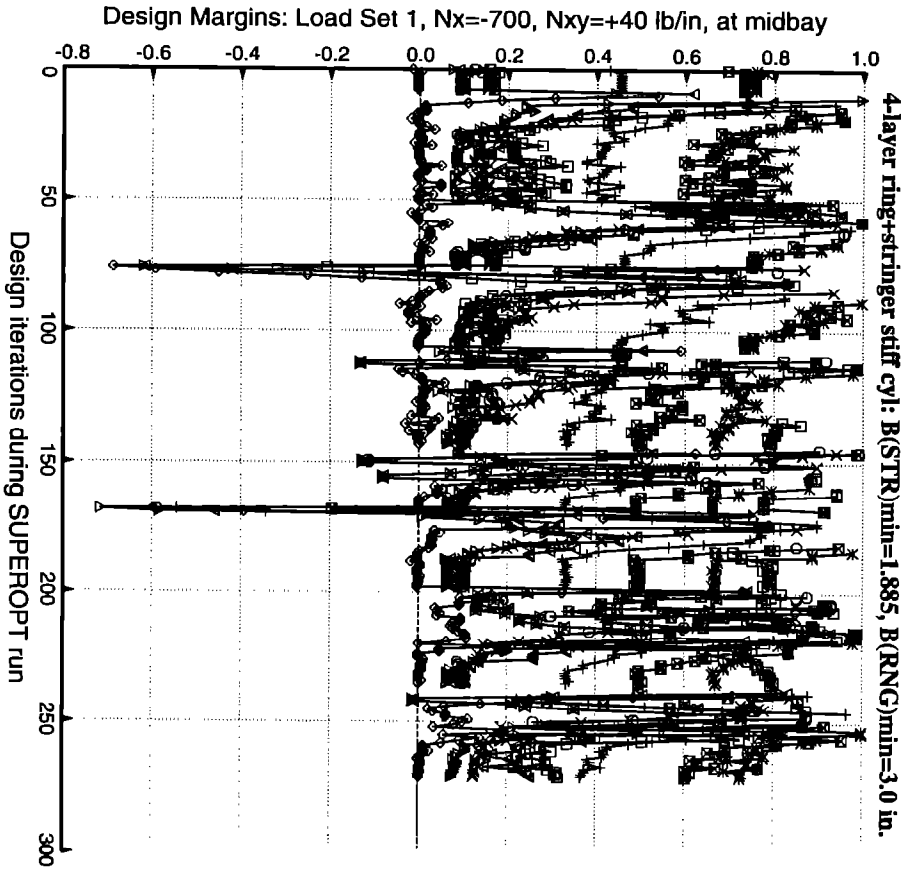

FIG. 24

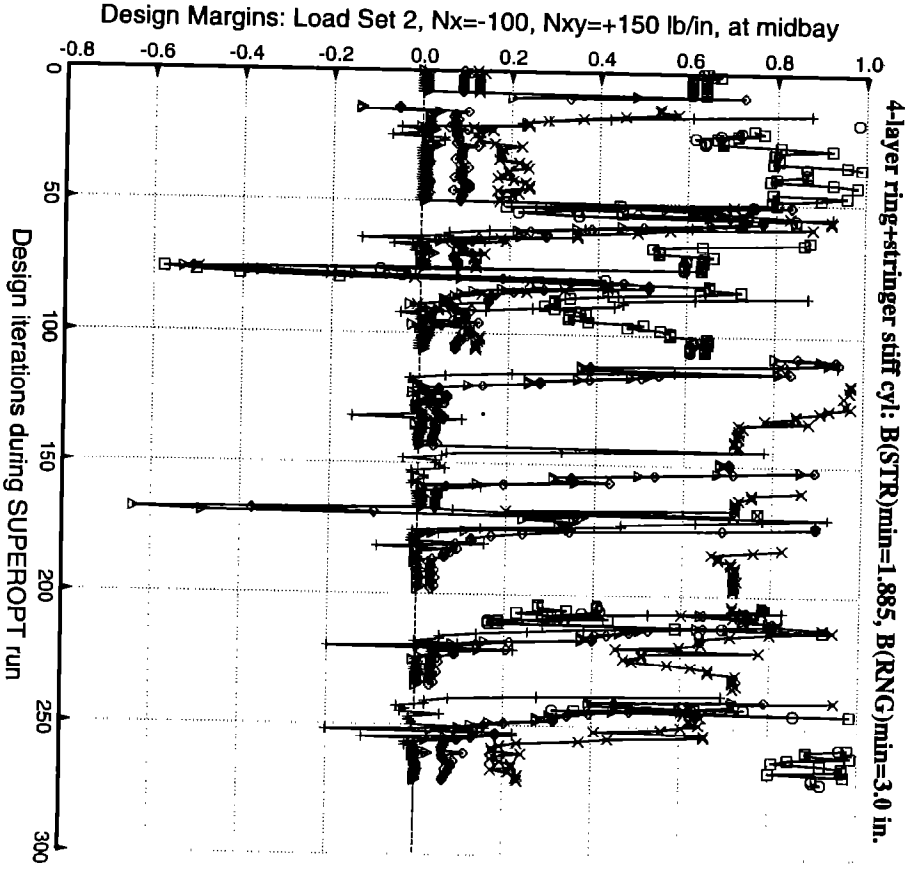

FIG. 25

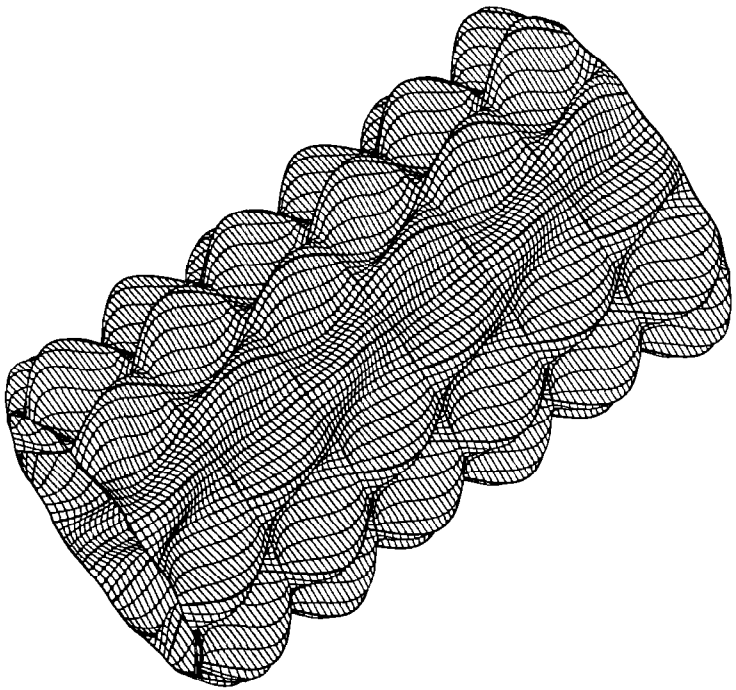

model scale = 0.1669E+01
, mode 1, pcr = 0.10304E+01
step 0 eigenvector deformed geometry
4-layer optimized ring+stringer-stiff. cyl: Nx=-700 lb/in, Nxy=+40 lb/in

FIG. 26

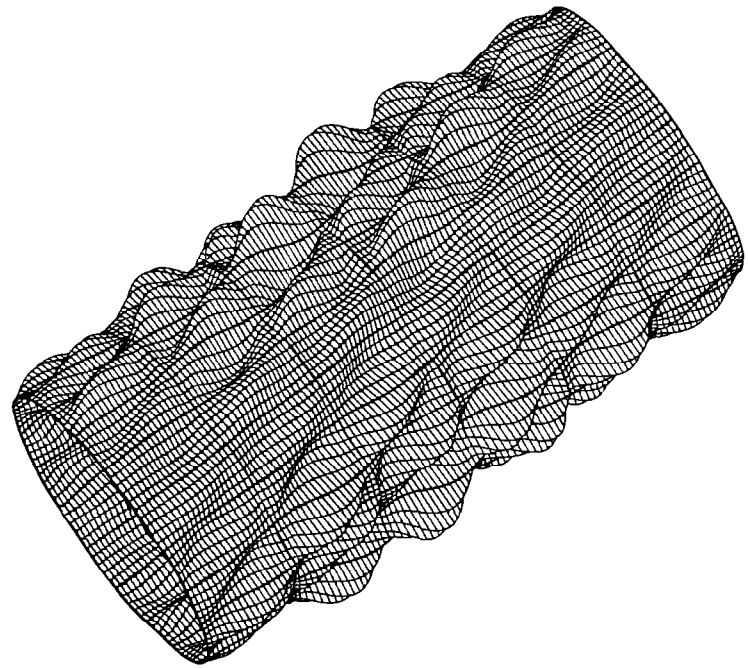

model scale = 0.1665E+01
, mode 1, pcr = 0.11326E+01
step 0 eigenvector deformed geometry
4-layer optimized ring+stringer-stiff. cyl: Nx=-100 lb/in, Nxy=+150 lb/in

FIG. 27

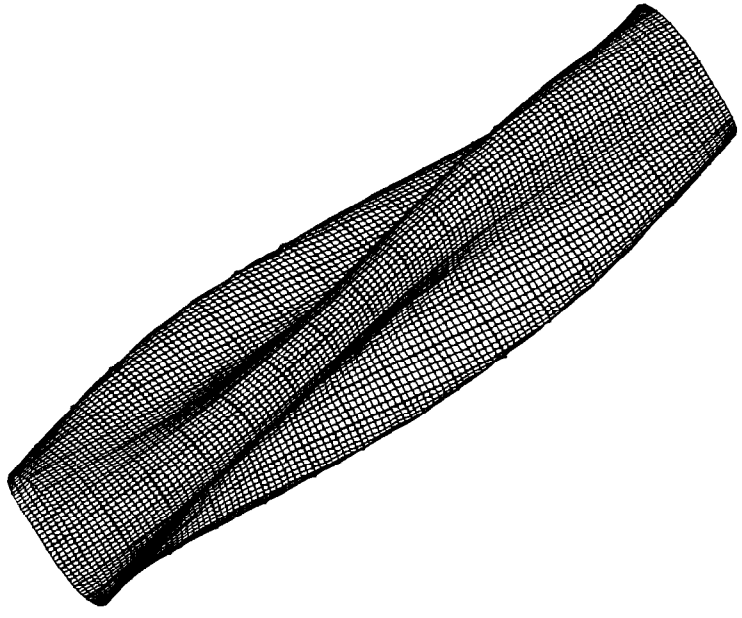

model scale = 0.3312E+01
, mode 1, pcr = 0.94698E+00
step 0 eigenvector deformed geometry
4-layer optimized ring+stringer-stiff cyl: Nx=-100 lb/in, Nxy=+150 lb/in

FIG. 28

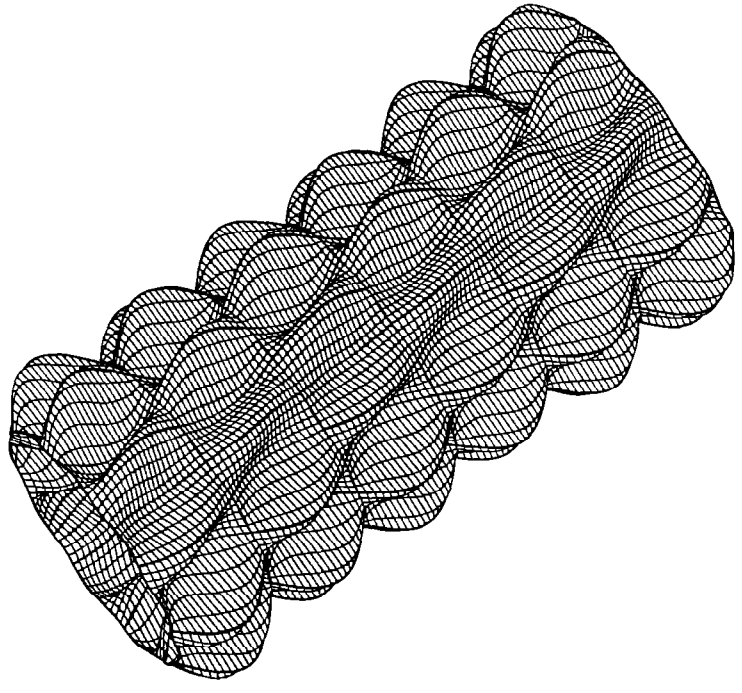

model scale = 0.1926E+01
, mode 1, pcr = 0.83716E+00
step 0 eigenvector deformed geometry
4-layer optimized ring+stringer-stiff. cyl: Nx=-700 lb/in, Nxy=+40 lb/in

FIG. 29

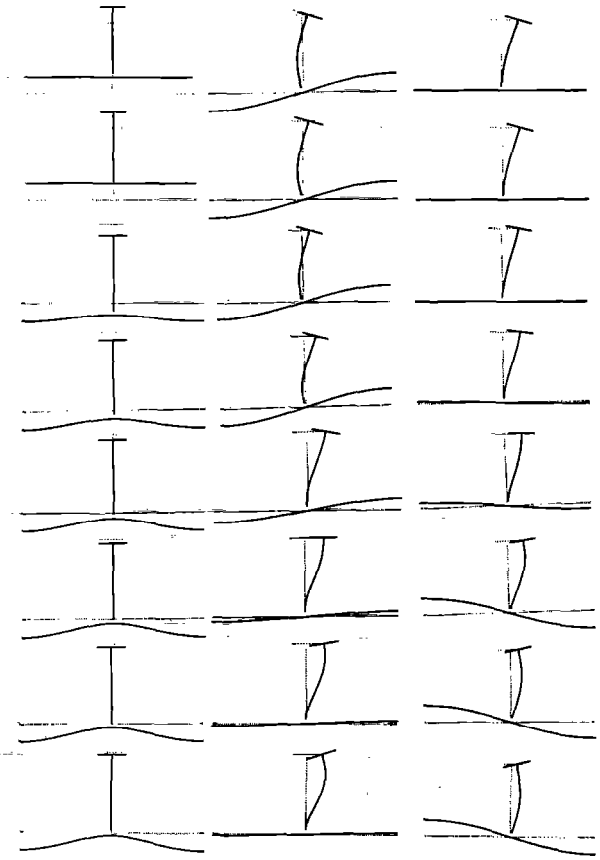

FIG. 30

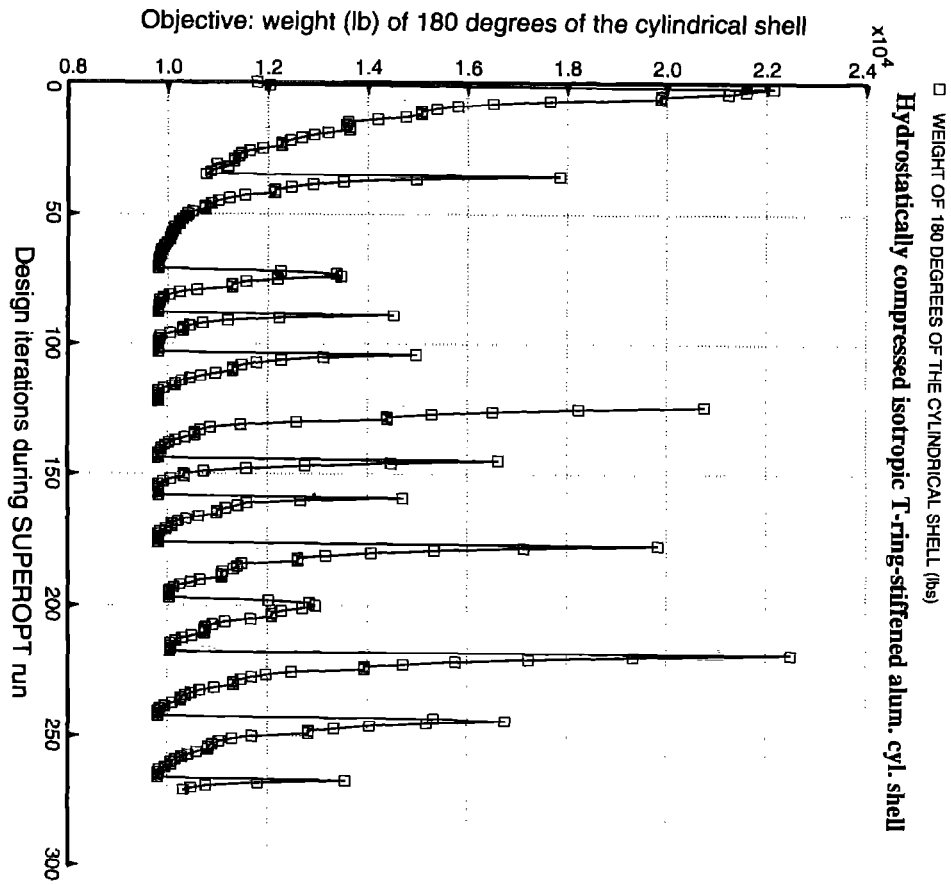

FIG. 31

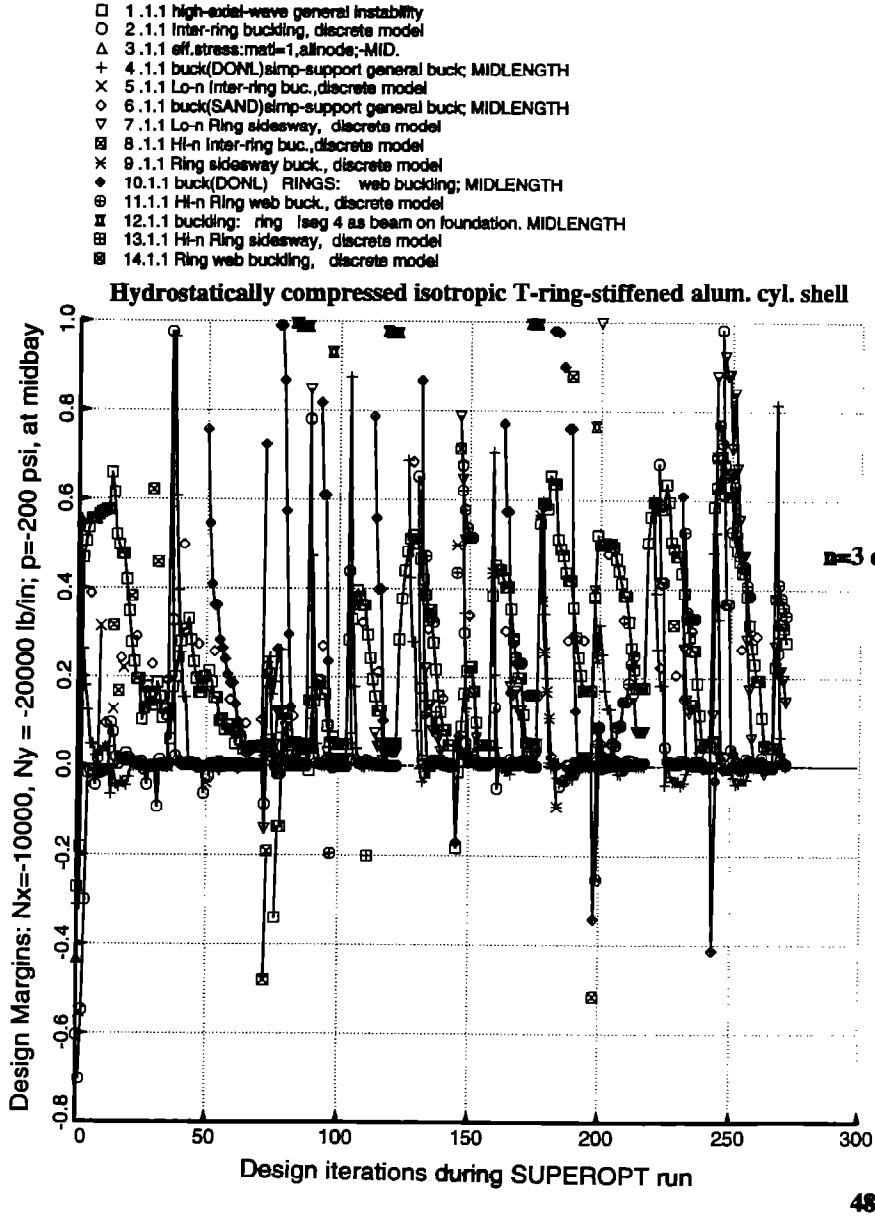

FIG. 32

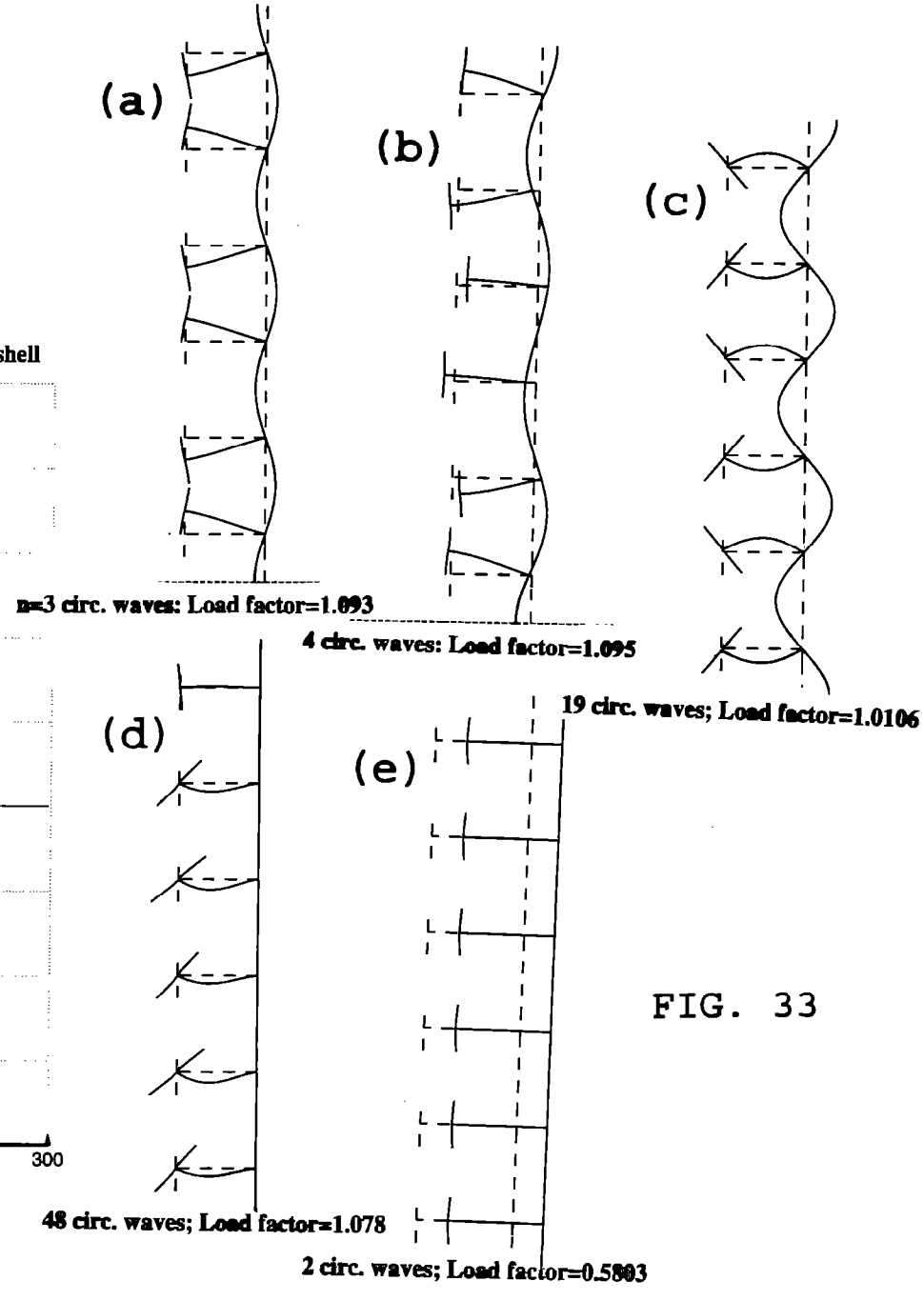

FIG. 33